ARTICLE

Regnase-1 is essential for B cell homeostasis to prevent immunopathology

Numana Bhat[1], Richard Virgen-Slane[3], Parham Ramezani-Rad[1], Charlotte R. Leung[1], Cindi Chen[1], Daniel Balsells[1], Ashima Shukla[1], Elaine Kao[1], John R. Apgar[1], Mingui Fu[2], Carl F. Ware[3], and Robert C. Rickert[1]

Regnase-1 is an emerging regulator of immune responses with essential roles in the posttranscriptional control of immune cell activation. Regnase-1 is expressed in B cells; however, its B cell–specific functions remain unknown. Here, we demonstrate that Regnase-1 prevents severe autoimmune pathology and show its essential role in maintaining B cell homeostasis. Using Cre driver mice for ablation of Regnase-1 at various stages of B cell development, we demonstrate that loss of Regnase-1 leads to aberrant B cell activation and differentiation, resulting in systemic autoimmunity and early morbidity. The basis of these findings was informed by gene expression data revealing a regulatory role for Regnase-1 in the suppression of a transcriptional program that promotes B cell activation, survival, and differentiation. Overall, our study shows that Regnase-1 exerts critical control of B cell activation, which is required for prevention of immunopathology.

Introduction

B cell responses are critical for effectively containing pathogens through antibody and cytokine secretion and by presenting antigens to T cells. Several checkpoints safeguard B cells to prevent inappropriate activation that may result in adverse immune reactions through self-antigen recognition and uncontrolled responses to foreign antigens (Nemazee, 2017). Various molecular mechanisms enable these checkpoints, such as the regulation of gene expression during B cell differentiation, which includes transcriptional and posttranscriptional control, and regulation of protein function and stability mediated by posttranslational modifications. These layers of molecular control are especially critical for maintaining B cell homeostasis and for affecting regulated responses through transitions between different stages of B cell development, activation, and differentiation. Different states of B cell activation are governed by distinct transcriptional programs that are mainly enabled by posttranscriptional regulation of mRNAs to allow rapid reprogramming of B cells during these transitions, while ensuring prevention of improper activation. RNA-binding proteins (RBPs) are the key players that facilitate these dynamic transcriptomic changes (Nutt et al., 2011; Turner and Díaz-Muñoz, 2018). Elucidating the function and underlying mechanisms of RBPs in the immune system is an active area of research, and the immunoregulatory roles of some RBPs have been studied in detail (Jeltsch and Heissmeyer, 2016; Kafasla et al., 2014). Although some RBPs have been shown to control B cell responses, the role of RBPs in the context of B cell regulation remains an emerging field of study.

Regnase-1 is an RBP that has been shown to control lethal inflammatory disease in mice (Matsushita et al., 2009). Regnase-1, encoded by the Zc3h12a gene, also known as monocyte chemotactic protein-inducible protein 1 (MCPIP-1), is essential for posttranscriptional control of immune cell activation. Regnase-1 destabilizes distinct sets of target mRNAs in different cell types, such as T cells, keratinocytes, and macrophages (Konieczny et al., 2019; Li et al., 2017; Matsushita et al., 2009; Uehata et al., 2013), suggesting cell type–specific immune regulation. In T cells, Regnase-1 is proteolytically cleaved by mucosa-associated lymphoid tissue lymphoma translocation protein 1 (MALT1), which is activated upon engagement of the T cell receptor, resulting in de-repression of critical effectors of T cell activation such as Il2 (IL-2), Tnfrsf4 (OX40), and Rel (c-Rel) mRNAs that are otherwise constitutively degraded by Regnase-1 during homeostatic conditions (Uehata et al., 2013). The canonical role of MALT1 had been established before this study as a critical component of the NF-κB pathway in lymphocytes (Ruefli-Brasse et al., 2003; Ruland et al., 2003). Antigen receptor engagement in both B and T lymphocytes triggers formation of a

protein complex consisting of CARMA1, BCL10, and MALT1, also known as the CBM complex (Thome et al., 2010). MALT1 plays a critical scaffolding role for formation of the CBM complex, which eventually results in nuclear translocation of NF-κB proteins (Lucas et al., 2001; Uren et al., 2000). NF-κB pathway activation up-regulates a transcriptional program that promotes lymphocyte functions including activation, proliferation, survival, and differentiation (Kaileh and Sen, 2012). Accordingly, MALT1 is essential for T cell–dependent humoral responses and germinal center (GC) formation (Ruefli-Brasse et al., 2003; Ruland et al., 2003).

GCs are microanatomically distinct structures in peripheral lymphoid organs that are formed by B cells during a T cell–dependent response to antigenic stimulation and are critical for mounting an effective humoral response and lasting immunological memory. During the GC reaction, B cells undergo proliferative expansion accompanied by multiple iterative cycles of somatic hypermutation and affinity-based selection, resulting in differentiation into memory B cells or high-affinity antibody-producing plasma cells (Mesin et al., 2016). In a previous study, we showed that MALT1 was required for GC B cell and plasma cell differentiation in a B cell–intrinsic manner with distinct roles in GC formation and plasma cell differentiation (Lee et al., 2017). Importantly, MALT1 was found to be proteolytically active in GC B cells, suggesting that MALT1 regulates GC B cells through its noncanonical activity mediated by proteolytic cleavage of target proteins (Lee et al., 2017). Interestingly, MALT1 also cleaves Regnase-1 in PMA-activated B cells ex vivo, suggesting that an immune regulatory mechanism similar to MALT1–Regnase-1 regulation of T cells may exist in B cells (Bornancin et al., 2015; Uehata et al., 2013). However, the role of Regnase-1 in B cells remains unexplored.

We sought to investigate the role of Regnase-1 in B cells by conditional gene inactivation of Regnase-1 at distinct stages of B cell development. Early deletion of Regnase-1 caused a strong immunopathological phenotype with aberrantly activated B cells. Acute ablation of Regnase-1 in B cells resulted in an augmented GC and antibody response to T cell–dependent antigens. RNA sequencing of Regnase-1–deficient B cells enabled identification of a Regnase-1–controlled transcriptional program that dampens B cell activation and differentiation. Deletion of Regnase-1 at later stages of B cell differentiation produced similar immunopathology to that observed upon early deletion of Regnase-1 during B cell development in the bone marrow. This study provides a first understanding of the fundamental role of Regnase-1 in the regulation of B cell differentiation and antibody responses.

Results

Regnase-1 is essential for preventing B cell–mediated immunopathology

Regnase-1 plays critical immunoregulatory roles in a cell type–specific manner. However, its function in B cells, a critical immune cell type that can mediate pathogenesis of immune-related disorders, is not known. Therefore, to study the B cell–specific role of Regnase-1, we selectively deleted Regnase-1 in B cells of

mice by using mice bearing homozygous floxed Regnase-1 (Zc3h12a) genes (Regnase-1[f/f]) that had been generated by flanking exon 3 of the Regnase-1 (Zc3h12a) gene with loxP sites (Li et al., 2017). We crossed the Regnase-1[f/f] mice with a mouse line with Mb1 (Cd79a)–driven expression of Cre recombinase (Hobeika et al., 2006), resulting in deletion of Regnase-1 during early B cell development in mice (referred to as the Regnase-1[f/f] Mb1[Cre] line henceforth). We observed that the Regnase-1[f/f] Mb1[Cre] mice had drastically reduced survival, with a median of 18 wk, compared with Regnase-1^{+/+} Mb1[Cre] controls (Fig. 1 A). The mice also had swollen abdomens and dermatitis (data not shown). Phenotypic characterization of Regnase-1[f/f] Mb1[Cre] mice revealed severe splenomegaly and lymphadenopathy (Fig. 1 B). Histological analysis showed disrupted follicular architecture in the secondary lymphoid organs (spleens, inguinal lymph nodes) as early as ∼8–10 wk of age (Fig. 1 C and Fig. S1 A). In addition, we observed leukocyte infiltration in the liver, which often occurs as a consequence of autoimmune and inflammatory diseases (Fig. 1 D; Hao et al., 2008; Kita et al., 2001).

Analysis of serum antibodies revealed hyperimmunoglobulinemia in Regnase-1[f/f] Mb1[Cre] mice compared with the control mice, with highly elevated levels of circulating antibodies of multiple isotypes (Fig. 1 E). Since the pathogenic antibodies that have been shown to be associated with various autoimmune and inflammatory disorders are of the class-switched IgG isotype (Holmdahl et al., 2019; Werwitzke et al., 2005), we further sought to characterize the circulating IgG antibodies from the sera of Regnase-1–deficient mice. We tested binding of the circulating IgG antibodies to a panel of antigens by ELISA, which showed polyreactivity to diverse antigens, such as insulin, cardiolipin, LPS, KLH, and DNA, compared with control mice (Fig. 1 F). In addition, kidneys from the diseased mice had high Ig deposition compared with the control animals (Fig. S1 B). Altogether, based on the phenotypic features of the Regnase-1[f/f] Mb1[Cre] mice, we conclude that Regnase-1 is essential for preventing B cell–driven immunopathology and hyperimmunoglobulinemia.

B cell–specific Regnase-1 deletion alters peripheral B cell populations and results in aberrant activation of B cells

Since Mb1-Cre–mediated deletion of Regnase-1 was specific to B cells, we assessed the B cell populations in the Regnase-1[f/f] Mb1[Cre] mice. We observed high cellularity in the secondary lymphoid organs, including the spleen and lymph nodes, with increased total number of B cells in Regnase-1[f/f] Mb1[Cre] mice compared with the control group (Fig. 2 A and data not shown). Increased cellularity was concomitant with a higher number of proliferating B cells as observed by the frequency of Ki67^{+}-staining CD19^{+} B cells in Regnase-1[f/f] Mb1[Cre] mice with respect to the control group (Fig. 2 A). The frequency of mature recirculating B cells that highly express B220 was strongly diminished in the spleens of Regnase-1[f/f] Mb1[Cre] animals (Fig. 2 B), although the absolute numbers were not significantly altered given the high total B cell numbers (Fig. S2 A). However, the relative frequency and the total number of B cells with downregulated surface B220 and up-regulated CD138 (B220^{int}CD138^{+}), associated with an activated or antibody-secreting phenotype, was significantly higher in the Regnase-1[f/f] Mb1[Cre] mice compared
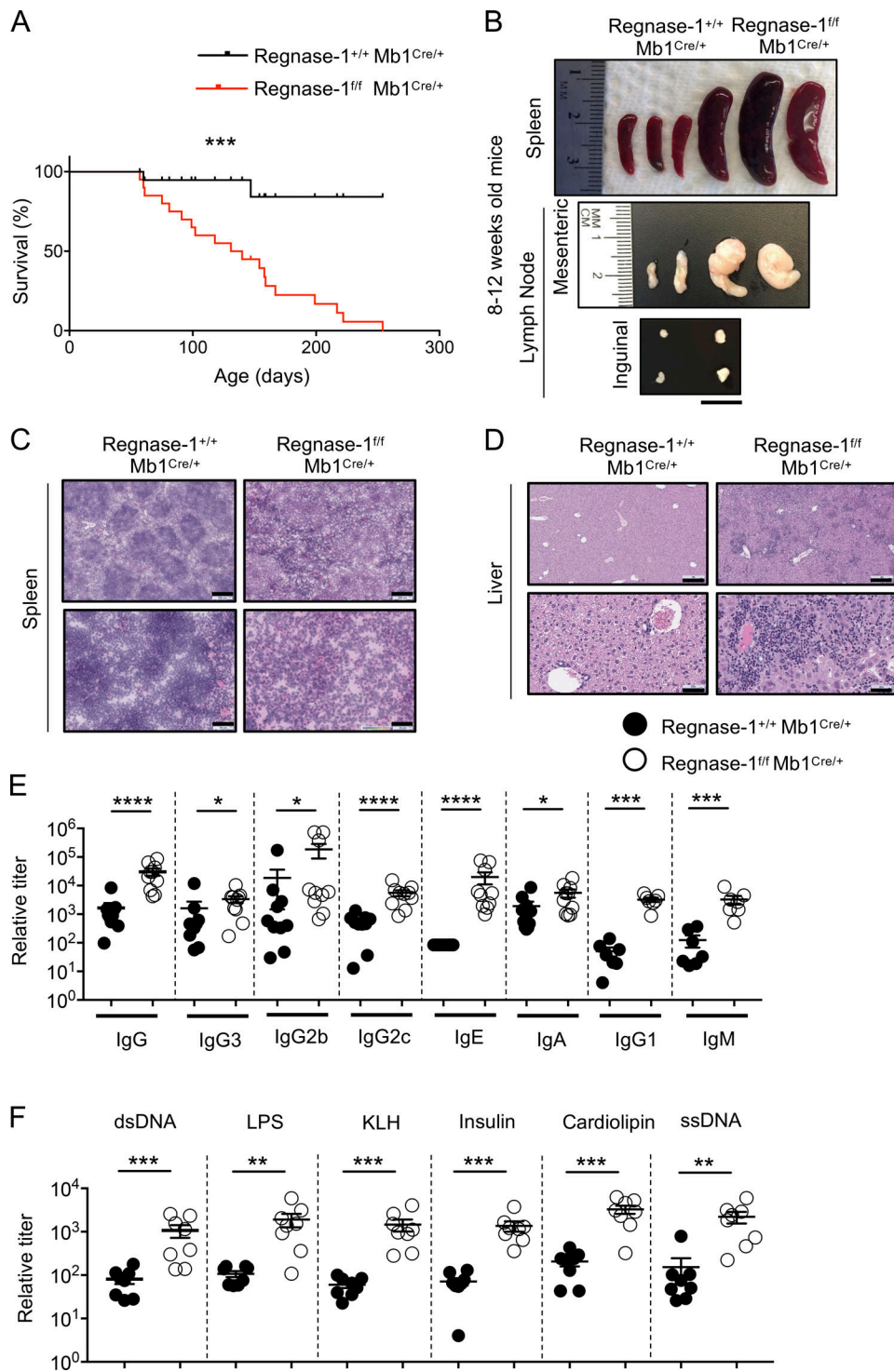
Figure 1. **Immunopathology in mice with B cell–specific deletion of Regnase-1. (A)** Survival plot of Regnase-1$^{f/f}$ Mb1$^{Cre/+}$ mice and Regnase-1$^{+/+}$ Mb1$^{Cre/+}$ controls at the indicated age in weeks (data pooled from two independent experiments; n = 10 in each). **(B)** Images of spleens and mesenteric and inguinal lymph nodes indicating splenomegaly and lymphadenopathy in Regnase-1$^{f/f}$ Mb1$^{Cre/+}$ mice (n = 3 mice; at least three independent experiments). Scale bar = 1 cm. **(C and D)** H&E staining of spleen (C) and liver (D). Scale bars = 250 μM (top), 50 μM (bottom) from the mice of indicated genotypes (n = 3–5 mice; two independent experiments). **(E)** Titers of total serum antibodies of different isotypes representing relative arbitrary units of measurement by ELISA. *P, < 0.05; ***, P < 0.001; ****, P < 0.0001. **(F)** Titers of antigen-specific serum antibodies of IgG isotype against indicated antigens representing relative arbitrary units of measurement by ELISA. **, P < 0.01; ***, P < 0.001. **(E and F)** Each symbol represents data from an animal; mean and standard deviation indicated by horizontal lines in the data points (n = 3–9 mice; two independent experiments); significance calculated by Mann-Whitney test. dsDNA, double-stranded DNA; ssDNA, single-stranded DNA.
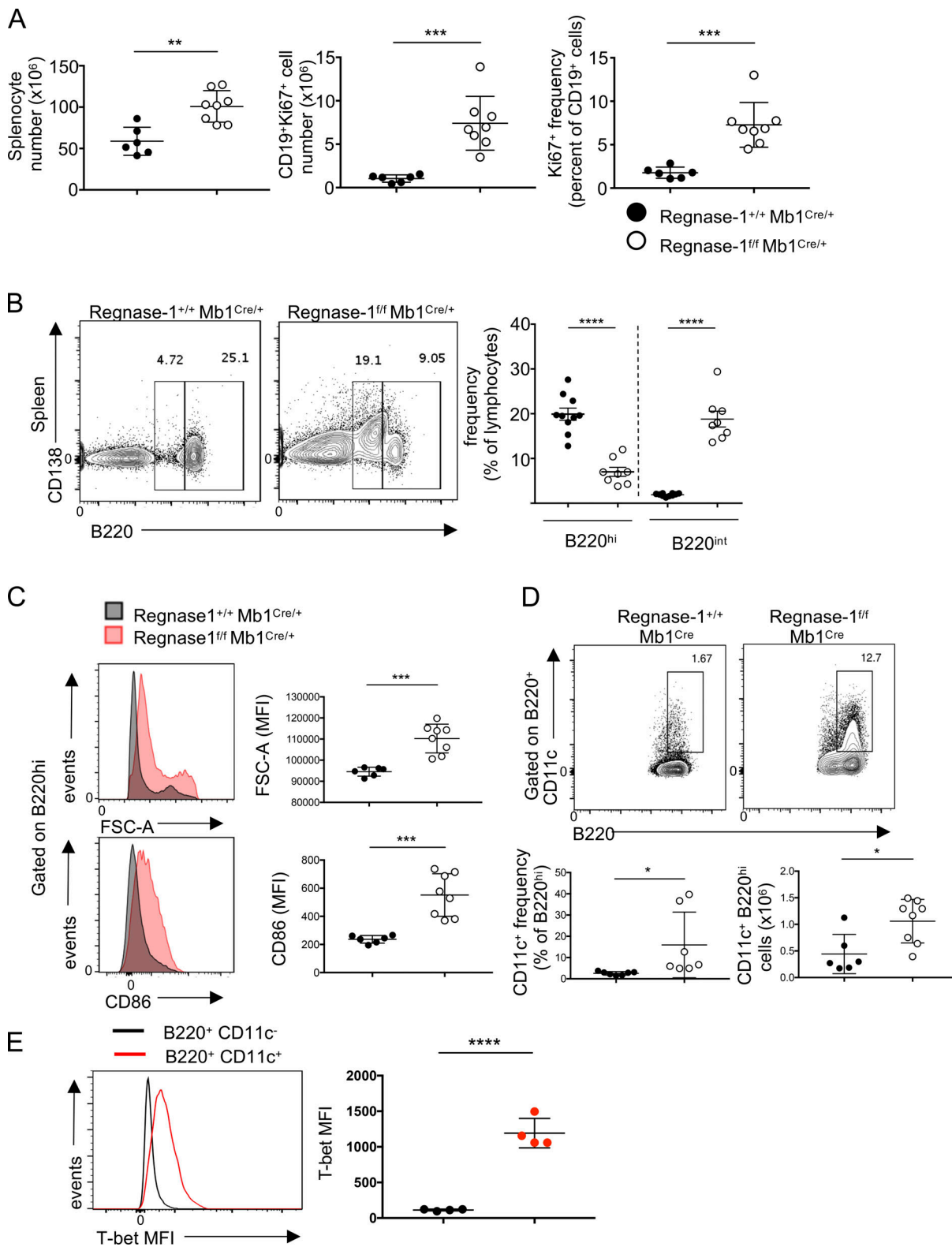
Figure 2. **Aberrant B cell populations in Regnase-1^{f/f} Mb1^{Cre} mice. (A and B)** Cellularity in spleens of mice of indicated genotypes (A) and flow cytometry dot plot showing B220 and CD138 staining to indicate an unusual B cell population (B220^{lo}CD138^{+}; B) in Regnase-1^{f/f} Mb1^{Cre} mice compared with Regnase-1^{+/+} Mb1^{Cre} controls. **(C)** Cell size of B220^{hi} B cells measured by forward scatter (FSC-A; top) and CD86 expression (bottom), both represented as MFI measured by flow cytometry. **(D)** Flow cytometry dot plots showing CD11c and B220 expression of B cells (gated on B220^{+} lymphocytes). **(A–D)** n = 3–9 mice; at least three independent experiments. **(E)** MFI measured by flow cytometry (n = 3 or 4 mice; two independent experiments). **(C and E)** Histogram events normalized to mode. **(A–E)** Each circle in the graph represents data from an animal; mean and standard deviation indicated by horizontal lines in the data points; significance calculated by unpaired Student's t test (*, P < 0.05; **, P < 0.01; ***, P < 0.001; ****, P < 0.0001).

with the controls (Fig. 2 B). In addition, B1a cell frequency in the peritoneal cavity and spleen of the Regnase-1[f/f] Mb1[Cre] mice was significantly reduced or absent (Fig. S2 F). We assessed the activation of the B220^{hi}CD138^{−} cells, the majority of which are naive in normal mice, to determine if these were prematurely activated in the Regnase-1[f/f] Mb1[Cre] mice and thus possibly a source of the "activated" B220^{int}CD138^{+} subset (Fig. 2 C). The size, as shown by the forward scatter, and the expression of activation markers such as CD86 were significantly higher in the B220[hi] B cell subset of the Regnase-1[f/f] Mb1[Cre] spleens (Fig. 2 C), showing that all cells are aberrantly activated upon B cell deletion of Regnase-1.

To further characterize B cell populations altered due to the loss of Regnase-1, we examined age-associated B cells (ABCs), a B cell subset that has been found to be strongly associated with ageing, autoimmunity, inflammation, and chronic viral infections in humans and animal models (Hao et al., 2011; Rubtsov et al., 2011). These cells are characterized by surface expression of CD11c, otherwise a conventional marker for dendritic cells, and are driven by a T-bet–mediated transcriptional program. Regnase-1[ff] Mb1[cre] mice displayed a significantly increased frequency of CD11c-expressing B cells compared with controls (Fig. 2 D). These cells also showed enhanced T-bet expression compared with CD11c^{−} B cells, determined by intracellular staining for T-bet (Fig. 2 E). The CD11c^{+} ABCs were discriminated from plasmacytoid dendritic cells, which are B220^{lo}CD11c^{+}, but also express Siglec-H and Gr-1 on the surface (Fig. S2 D).

Thus, we show that the B cell–specific deletion of Regnase-1 results in strong alterations in B cell maturation, causing aberrant activation of B cells and a high frequency of abnormal B cell subpopulations such as B220^{lo}CD138^{+} B cells and ABCs in the spleen.

Regnase-1 regulates a transcriptional program associated with B cell activation

Regnase-1 as an RBP has been shown to regulate the transcriptomes of immune cells, particularly T cells (Uehata et al., 2013; Wei et al., 2019); therefore, we sought to analyze the transcriptome of Regnase-1–deficient B cells to understand the molecular mechanism of Regnase-1–mediated regulation in B cells. As discussed above, early deletion of Regnase-1 at the pro–B cell stage resulted in a striking immunopathological phenotype, thus precluding precise analysis of B cell–specific molecular functions of Regnase-1. In addition, the chronic effect of Mb1-Cre–dependent Regnase-1 ablation strongly altered the surface expression of various B cell markers, making it challenging to isolate and perform ex vivo studies on B cells (Fig. S2 E). To circumvent these issues resulting from the severe immunopathology that we observed, we generated an inducible deletion model of Regnase-1 by crossing Regnase-1[f/f] mice to a mouse line in which Cre recombinase expression is driven by a human transgene, hCD20. In these mice, referred to as Regnase-1[f/f] hCD20Tam[Cre], Cre recombinase is expressed in mature B cells and is functionally activated by tamoxifen (Khalil et al., 2012), thus enabling proper assessment of B cell–specific roles of Regnase-1 upon acute deletion.

We performed RNA sequencing (RNA-seq) analysis of B cells isolated from tamoxifen-administered Regnase-1[f/f] hCD20Tam[Cre] and control mice. B cells isolated from the Regnase-1[f/f] hCD20Tam[Cre] mice showed diminished Regnase-1 expression

(Fig. S3 A and Fig. S3 B). Pathway enrichment analysis showed highly significant impacts to pathways and cellular processes such as cell cycle regulation, dysregulation of GC response and other autoimmune-associated pathways, inflammatory signaling involving IL-1, IL-2, macrophage migration inhibitory factor, and survival signatures associated with B cell receptor (BCR) signaling, TNF, Bcl2, and NF-κB pathway (Fig. 3 A and Table S1). With further analysis for differentially expressed genes (DEGs) using an adjusted P value of 0.1, we detected ∼200 genes with significant differential expression in Regnase-1–deficient B cells. The top 80 genes among the DEGs are displayed in the heatmap showing their normalized expression, scaled by row (Fig. 3 B). As expected, Regnase-1 itself (Zc3h12a) was found among the significantly down-regulated genes. Interestingly, IL receptors for Il2 (IL-2), Il4 (IL-4), and Il21 (IL-21) were down-regulated upon Regnase-1 deletion. Among the top up-regulated genes in the Regnase-1–deficient B cells were TACI (transmembrane activator and CAML interactor, or Tnfrsf13b), which is a receptor for B cell survival factors such as BAFF (B cell activating factor) and APRIL (a proliferation-inducing ligand; Mackay and Schneider, 2009). TACI is normally up-regulated on antibody-secreting cells and is critical for class switching (Castigli et al., 2005; He et al., 2007). In addition, TACI expression is increased in the B cells of patients with autoimmune diseases such as lupus nephritis, and deletion of TACI in systemic lupus erythematosus mouse models such as BAFF transgenic mice ameliorates the disease (Arkatkar et al., 2018; Figgett et al., 2015). Bcl2, also among the up-regulated genes, is a critical survival factor in B cells, but its high expression can promote autoimmune diseases (Strasser et al., 1991). In addition, Nfkbiz, whose role in B cells is not well studied but has been shown to be a substrate of Regnase-1 in HeLa cells, was up-regulated (Behrens et al., 2018). Interestingly, Regnase-4 (Zc3h12d), a tumor suppressor gene from the same family of RNases as Regnase-1, was up-regulated, suggesting a potential compensatory role of Regnase-4 upon Regnase-1 deficiency and thus a possible overlap in the functions of different Regnase family members (Minagawa et al., 2014). Notably, some other genes of interest among the top 80 DEGs that have a previously established immunomodulatory role in B cells were Zfp36l1, Fcgr2b, Cd72, Ikzf1, and Pou2f2.

The above analysis enabled assessing the transcriptional program regulated by Regnase-1 in B cells under steady state. However, engagement of the BCR is crucial for B cell activation that results in several changes, leading to the induction of a transcriptional program involved in activation, proliferation, and differentiation. BCR engagement involves up-regulation of genes associated with the NF-κB pathway orchestrated by the BCR-induced assembly of the CBM complex. Given that TCR activation induces proteolytic cleavage of Regnase-1, we hypothesized that BCR activation could lead to similar changes in B cells (Uehata et al., 2013). To test this hypothesis, we stimulated primary mouse B cells with anti-IgM F(ab′)2 and observed rapid cleavage of Regnase-1 (Fig. 4 A). This could be mediated by the proteolytic activity of MALT1 (Bornancin et al., 2015), as was also indicated by probing for Regnase-1 levels in B cells from germline-deficient MALT1^{−/−} mice (Fig. S4 A). The rapid cleavage of Regnase-1 upon BCR activation suggests its possible role in
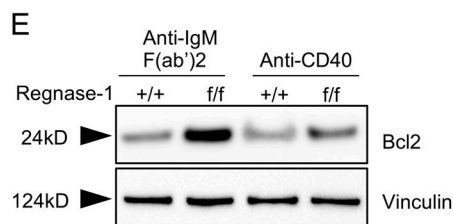
A

Pathway Maps (−log (pValue), 0 to 15):
- Immune response_TNF-R2 signaling pathways
- Apoptosis and survival Anti-apoptotic TNFs/NF-κB/Bcl-2 pathway
- B cell signaling in hematological malignancies
- Dysregulation of germinal center response in SLE
- Immune response_IL-3 signaling via JAK/STAT
- Signal transduction_CXCR4 signaling via MAPKs cascades
- Apoptosis and survival_APRIL and BAFF signaling
- Immune response_IL-1 signaling pathway
- Role of IFN-beta in the improvement of blood-brain barrier integrity in multiple sclerosis
- TNF-α and IL-1 β-mediated regulation of contraction and secretion of inflammatory factors in normal and asthmatic airway smooth muscle

Process Networks (−log (pValue), 0 to 10):
- Immune response_BCR pathway
- Cell cycle_G1-S Interleukin regulation
- Inflammation_IL-2 signaling
- Immune response_Phagocytosis
- Immune response_TCR signaling
- Inflammation_MIF signaling
- Cell cycle_G1-S Growth factor regulation
- Inflammation_IL-10 anti-inflammatory response
- Proliferation_Lymphocyte proliferation
- Inflammation_Neutrophil activation

B

Genes (top cluster): Itgb3, Fos, Pik3cg, Arhgap31, Gramd3, C230081A13Rik, Lax1, Zc3h12a, Tagap, Eif2c2, Zfp36l1, Dusp5, Neil1, Eng, Foxp4, 4933407C03Rik, Rgs2, Snrnp25, Pou2af1, Rara, Zbtb46, Antxr2, Il21r, Lrrc8d, Csrp2, Dusp1, Zfp36, B4galnt1, Rrad, Nfkb2, Fpgs, Vps37b, P2ry10, 1700017B05Rik, Tmem123, Junb, Cables1, Il4ra, Flnb, Rnf125, Il2rg, Smad7

Genes (bottom cluster): Pdia4, Fam129c, Ncf1, Grm6, Tnfaip8, Cd244, Cdk5rap1, Gbp5, Dcp2, Fcgr2b, Cd72, Atp2a3, Fcrl5, Cd38, Aldh2, Suclg2, Ikzf1, Adam19, Slit3, Heatr6, Zc3h12d, Ceacam1, Pikfyve, Pecam1, Bmf, Bcar3, Abcc4, Il10ra, Tnfrsf13b, Bcl2, Gbp3, Nup210, Sema4b, Pou2f2, Nfkbiz, Sh3bp5, Anp32a, Fam111a

Regnase-1 +/+ hCD20TamCre   Regnase-1 f/f hCD20TamCre

C

■ Regnase-1 +/+ hCD20TamCre
□ Regnase-1 f/f hCD20TamCre

Relative *Tnfrsf13b* mRNA (normalized to *Gapdh*)

Relative *Bcl2* mRNA (normalized to *Gapdh*)

D

Regnase1+/+ hCD20TamCre
Regnase1f/f hCD20TamCre

events — TACI (*Tnfrsf13b*) MFI

****

Regnase-1 +/+ hCD20TamCre   Regnase-1 f/f hCD20TamCre

E

Regnase-1: Anti-IgM F(ab')2 (+/+, f/f), Anti-CD40 (+/+, f/f)
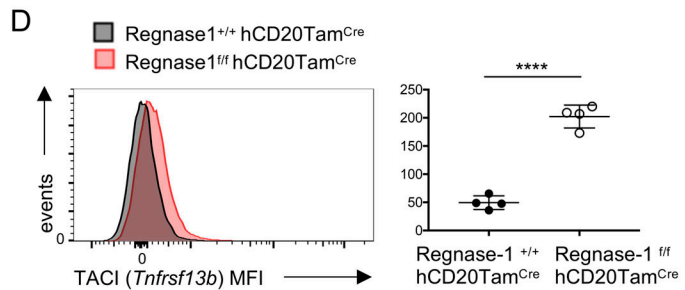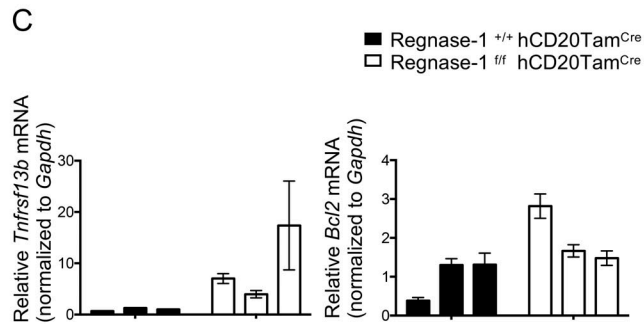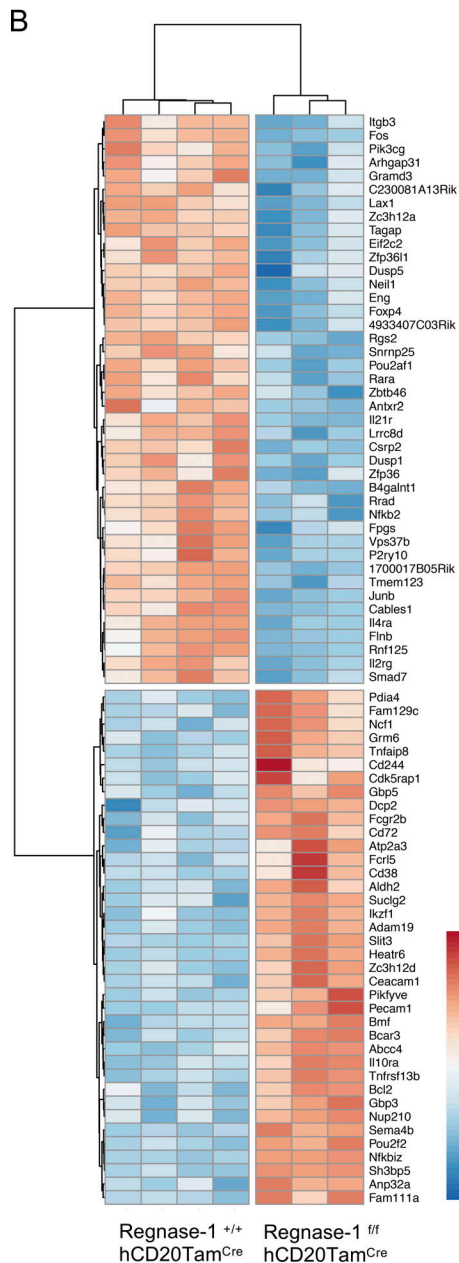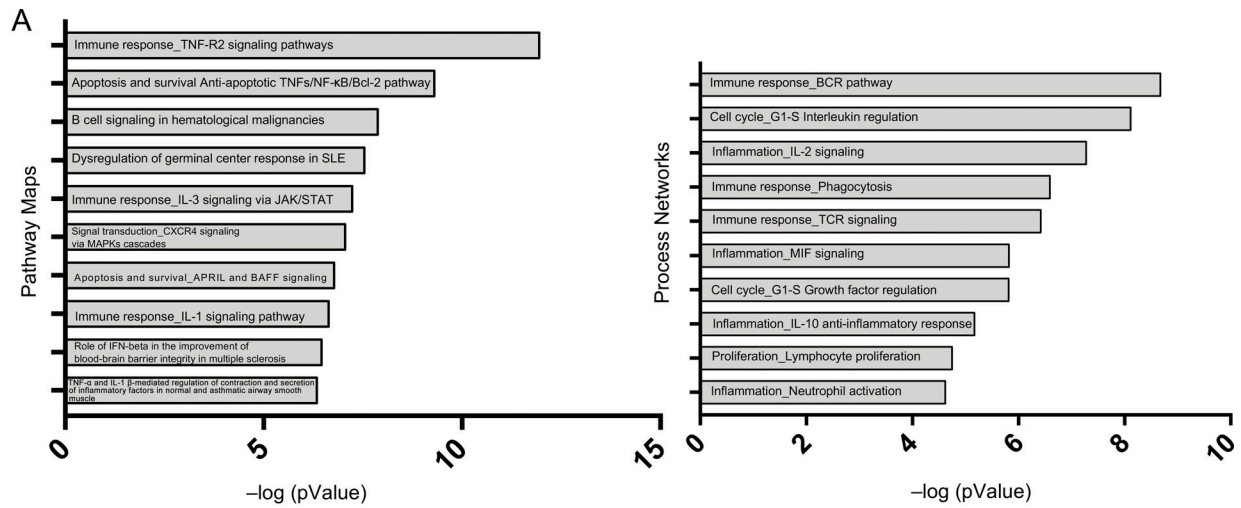
24kD ▸ Bcl2
124kD ▸ Vinculin

Figure 3. Regnase-1 regulates a B transcriptional program that promotes B cell activation, survival, and differentiation. (A) Pathway maps and process networks from RNA-seq that are enriched in B cells isolated from Regnase-1$^{f/f}$ hCD20Tam^{Cre} compared with Regnase-1$^{+/+}$ hCD20Tam^{Cre} B cells. Bars represent −log of P values for enrichment calculated in Metacore. **(B)** Heatmap showing top 80 differentially expressed transcripts in Regnase-1$^{f/f}$ hCD20Tam^{Cre} B cells. Each column represents data from one animal. Scale bar represents Z scores of DESeq2-normalized expression, scaled by row. **(A and B)** n = 3 or 4 animals; RNA-seq experiment performed once. **(C)** Fold change of mRNA levels of Tnfrsf13b (left) and Bcl2 (right) in Regnase-1$^{f/f}$ hCD20Tam^{Cre} compared with Regnase-1$^{+/+}$ hCD20Tam^{Cre} B cells. Bars represent mean and standard deviation of fold changes from experimental triplicates; each bar represents data from one animal (n = 2–4 mice; two independent experiments). Expression levels of the tested transcripts have been normalized to levels of GAPDH mRNA control for each data point. **(D)** Tnfrsf13b expression shown as MFI measured by flow cytometry. Histogram represents data from four animals per group, also plotted in the graph (right). Histogram events normalized to mode. n = 2–4 mice; two independent experiments. Horizontal lines indicate means with SD shown by the error bars. ****, P < 0.0001. **(E)** Western blot showing Bcl2 protein levels and Vinculin (loading control) in B cells from the mice of indicated genotypes when stimulated with anti-IgM F(ab')2 or anti-CD40. +/+ = Regnase-1$^{+/+}$ hCD20Tam^{Cre}; f/f = Regnase-1$^{f/f}$ hCD20Tam^{Cre} (n = 2 mice; two independent experiments). **(A–E)** Mice were administered tamoxifen i.p. for 5 consecutive d; B cells isolated on day 11 after first dose. MAPK, mitogen-activated protein kinase; MIF, macrophage migration inhibitory factor; SLE, systemic lupus erythematosus.

---

modulating BCR-induced genes (Fig. 4 A). Accordingly, to identify potential BCR-responsive genes that may be modulated by Regnase-1, we performed a transcriptome analysis of B cells from Regnase-1$^{f/f}$ hCD20Tam^{Cre} mice that were stimulated with anti-IgM F(ab')2. As shown in Fig. 4 B, the transcriptome analysis revealed several genes that show significant differential expression in the stimulated Regnase-1–deficient B cells. Principal component analysis using regression coefficients revealed increased expression of certain genes that have been previously shown to be important for B cell survival and differentiation (Fig. 4 C). These include genes such as Batf, Tnfrsf13b, and Bcl2, which were significantly enhanced upon BCR stimulation of Regnase-1–deficient B cells (Fig. 4 C). The differential expression of some of the genes of our interest among the top DEGs at steady state or upon BCR stimulation, such as Bcl2, Tnfrsf13b, Batf, Gpr183, Nfkbiz, and Ikzf1, were validated by RT-qPCR (RT and quantitative PCR; Fig. 3 C, Fig. 4 D, and Fig. S3 D). Also, the surface expression of Tnfrsf13b (TACI) was measured by flow cytometry, and Bcl2 expression was examined by immunoblotting, and both were higher in Regnase-1–deficient B cells compared with controls (Fig. 3 D). The top DEG in BCR-stimulated, Regnase-1–deficient B cells was Batf, and interestingly, Wei et al. (2019) recently showed that Batf is an important target and a direct substrate of Regnase-1 that promotes anti-tumor activity of tumor-infiltrating T cells. Among the top DEGs, Batf and Zfp36l1 appeared to be posttranscriptionally regulated by Regnase-1 in B cells (Fig. S3 C). In B cells, Batf is known to be essential for activation-induced cytidine deaminase (AID) expression and isotype class switching, suggesting a possible role of Regnase-1 in controlling these B cell processes (Betz et al., 2010; Ise et al., 2011).

Thus, Regnase-1 controls a transcriptional program in B cells that is associated with survival, activation, and differentiation and regulates the expression of a set of genes that are induced upon BCR stimulation.

Regnase-1 plays a role in controlling B cell growth potential and B cell differentiation into class-switched B cells

During progression of autoimmune disorders, pathogenic antibodies present as switched isotypes, mostly IgG subtypes, while IgM has been associated with a protective role (Holmdahl et al., 2019; Werwitzke et al., 2005). Given that the top up-regulated genes in the transcriptome analysis promote B cell differentiation, we sought to determine if Regnase-1–deficient B cells have

an increased propensity for activation and class switching. To test if BCR signaling was impacted in the absence of Regnase-1, we determined the change in intracellular calcium levels upon BCR stimulation and observed that calcium signaling in Regnase-1–deficient B cells appears intact upon BCR stimulation (Fig. S4 B). We also studied the effect of Regnase-1 deletion on B cell growth, proliferation, and class switching in response to various stimuli. Class switching to the IgG3 subtype upon LPS stimulation and to the IgG1 isotype with stimuli that mimic T cell help was significantly higher in B cells from Regnase-1$^{f/f}$ hCD20Tam^{Cre} mice compared with controls (Fig. 5 A). B cells from the Regnase-1$^{f/f}$ hCD20Tam^{Cre} were much bigger than the B cells from the Regnase-1$^{+/+}$ hCD20Tam^{Cre} control B cells, and the increased cell size was further pronounced upon BCR stimulation or treatment with anti-CD40, recombinant IL-4, and recombinant BAFF (Fig. 5 B). In addition, B cells from Regnase-1$^{f/f}$ hCD20Tam^{Cre} mice proliferated modestly higher upon BCR and TLR4-stimulation or when signals (such as stimulatory anti-CD40 antibody and IL4) that mimic T cell help were provided (Fig. 5 B). Thus, Regnase-1 plays a role in differentiation into class-switched B cells and B cell growth and proliferation.

Regnase-1 controls B cell differentiation in the GC

We used gene expression data extracted from the Immgen RNA-seq database to identify genes that were enriched in GC B cells compared with resting follicular B cells. Gene set enrichment analysis (GSEA) led to identification of genes that were elevated in the BCR-stimulated Regnase-1–deficient B cells in our RNA-seq analysis, as detected by using a Generalized Linear Model (~ Stimulation + Stimulation:Genotype), and were found to be significantly enriched in the GC B cell genes from the Immgen RNA-seq data (Fig. 6 A and Fig. S4 B). In contrast, the genes from the BCR-stimulated Regnase-1–deficient B cells were down-regulated in follicular B cell genes in the Immgen dataset (Fig. 6 A and Fig. S4 B). However, the genes associated with unstimulated Regnase-1–deficient B cells did not show any significant relationships with the reference gene sets (adjusted P value >0.1; data not shown). This suggested that Regnase-1 suppresses a GC-like signature in activated B cells. In addition, we probed by immunoblotting for Regnase-1 protein expression in follicular B cells and GC B cells and found that Regnase-1 expression was strongly down-regulated in GC B cells (Fig. 6 B). This suggested a role for Regnase-1 in B cells during the GC reaction.
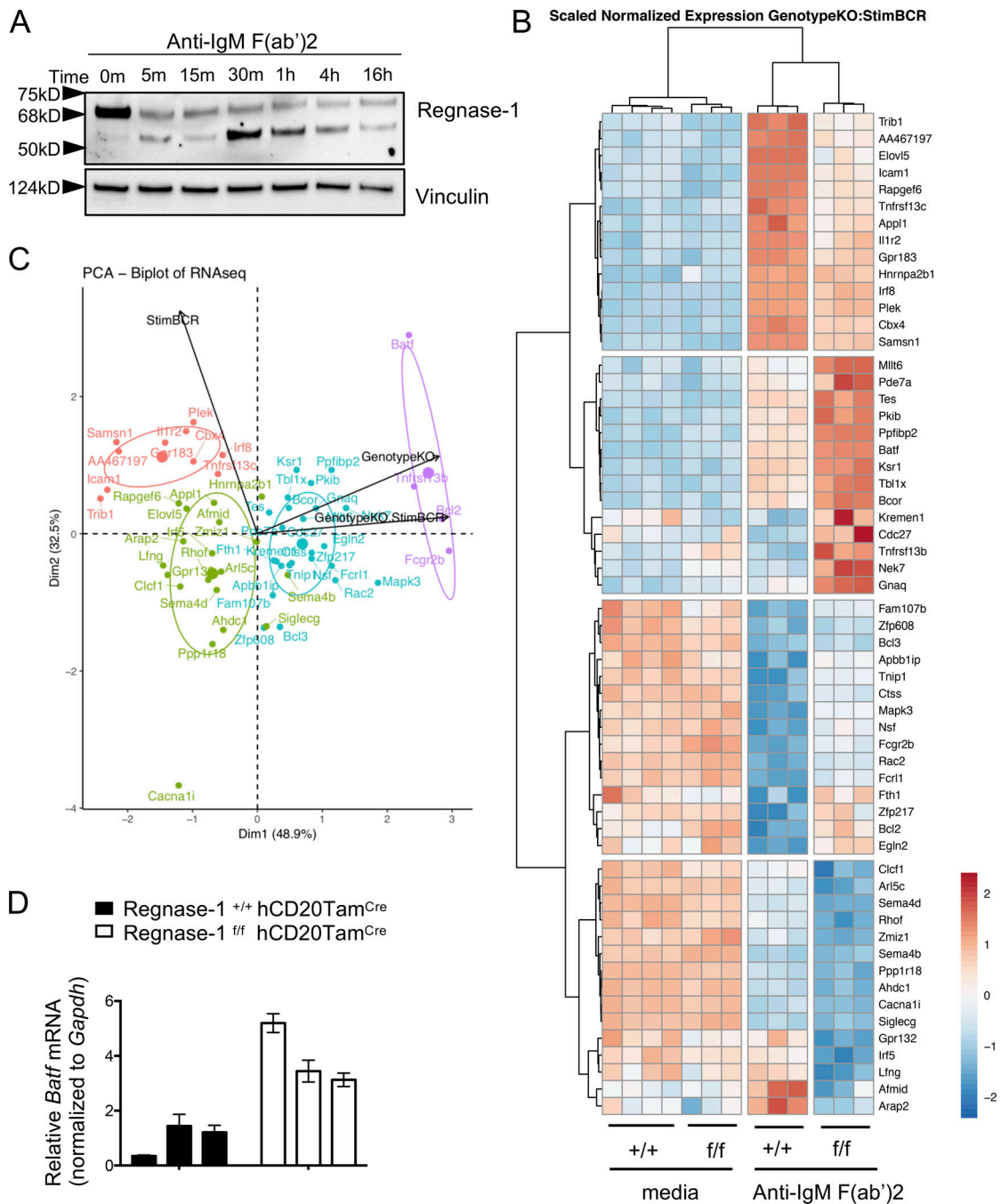
Figure 4. **Regnase-1–mediated regulation of BCR-driven transcriptome changes. (A)** Western blot showing Regnase-1 cleavage upon BCR stimulation of splenic B cells for the indicated time points (data representative of three independent experiments). **(B)** Heatmap showing genes with significant differential expression in BCR-stimulated, Regnase-1–deficient B cells. Each column represents DESeq2-normalized expression data from one animal. Scale bar represents Z scores of normalized expression, scaled by row. GenotypeKO, Regnase-1^f/f hCD20Tam^Cre; StimBCR, anti-IgM stimulated condition; +/+, Regnase-1^+/+ hCD20Tam^Cre; f/f, Regnase-1^f/f hCD20Tam^Cre. **(C)** Principal component analysis plot generated for genes with significant differential expression in BCR-stimulated, Regnase-1–deficient B cells. Arrows correlated with fold change of gene expression for the indicated contrasts, reported from DESeq2 regression coefficients. **(B and C)** n = 3 or 4 animals; RNA-seq performed once. **(D)** Fold change of Batf mRNA levels in Regnase-1^f/f hCD20Tam^Cre compared with Regnase-1^+/+ hCD20Tam^Cre B cells. Bars represent the mean and standard deviation of fold changes from experimental triplicates; each bar represents data from one animal (representative of two independent experiments). Batf mRNA levels normalized to GAPDH control for each data point. **(B–D)** Mice were administered tamoxifen i.p. for 5 consecutive d; B cells isolated on day 11 after first dose.

To test the role of Regnase-1 in GC B cells, we immunized Regnase-1^f/f hCD20Tam^Cre and Regnase-1^+/+ hCD20Tam^Cre control mice with sheep RBCs (SRBCs) and analyzed T cell–dependent responses on day 6 after immunization. Regnase-1^f/f

hCD20Tam^Cre mice showed an enhanced GC response with a higher frequency of GC B cells (B220^+GL7^+Fas^+) compared with control mice (Fig. 6 C). From the RNA-seq analysis, the top upregulated mRNA in BCR-stimulated Regnase-1–deficient B cells
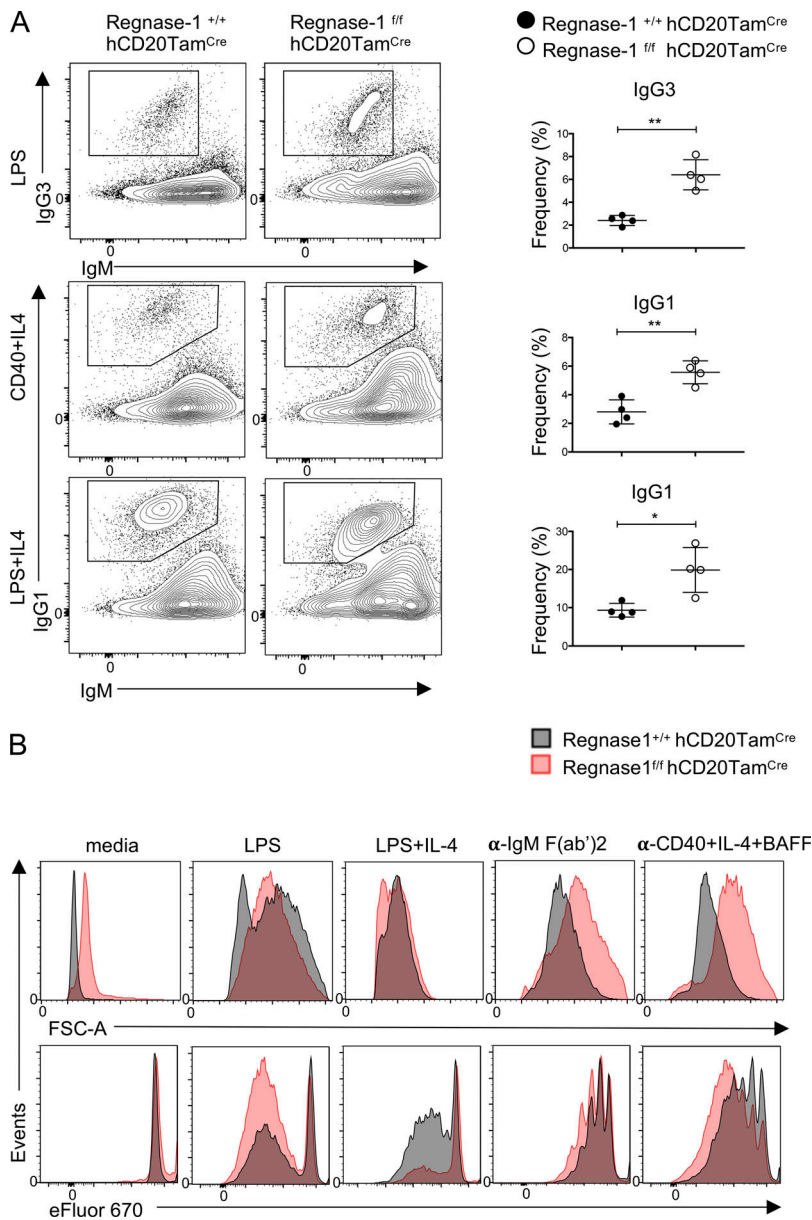
Figure 5. **Regnase-1 regulates B cell class switching and cell growth. (A)** Representative flow cytometry plots showing class switching to IgG1 and IgG3 with indicated stimuli. Data from four animals per group plotted as frequencies (percentage) on the right. Horizontal lines indicate means with SD shown by error bars. Statistical significance calculated by unpaired Student's t test (*, P < 0.05; **, P < 0.01). **(B)** Cell size (top) of B cells measured by forward scatter (FSC-A) and proliferation (bottom) measured by eFluor 670 dilution, both represented as MFI measured by flow cytometry. Events in the histograms are normalized to mode. **(A and B)** Mice were administered three doses of tamoxifen i.p. on alternate days; B cells isolated on day 11 after first dose. Data representative of three independent experiments; n = 2–4 mice in each.

was the transcription factor *Batf*, which, in addition to being essential for AID expression and class switching (Betz et al., 2010; Ise et al., 2011), is also critical for entry of B cells from the light zone (LZ) into the dark zone (DZ) phase of the GC reaction (Inoue et al., 2017). Therefore, we determined the effect of Regnase-1 deletion on the distribution of B cells between the LZ and DZ. SRBC-immunized Regnase-1$^{f/f}$ hCD20Tam^{Cre} mice displayed a higher relative frequency of DZ B cells with respect to LZ B cells (DZ/LZ ratio) compared with controls as determined by enumerating CXCR4^{hi}CD86^{lo} and CXCR4^{lo}CD86^{hi} GC B cells, respectively (Fig. 6 C). This observation indicates that Regnase-1 may possibly play a role in the regulation of interzonal cycling of B cells. In addition, the frequency of plasma cells (B220^{lo}CD138^{hi}) was significantly higher in Regnase-1$^{f/f}$ hCD20Tam^{Cre} mice (Fig. 6 C), showing that Regnase-1 has a role in differentiation of B cells into antibody-secreting cells. To determine if the antibody response was altered, we measured antibody titers in

the sera of Regnase-1$^{f/f}$ hCD20Tam^{Cre} and control mice. Circulating antibodies were elevated in Regnase-1$^{f/f}$ hCD20Tam^{Cre} mice, particularly the antibodies of the switched isotypes (Fig. 6 D), consistent with increased isotype switching observed in vitro (Fig. 5 A). Further characterization of the antigen-specific antibody response in the immunized mice showed elevated SRBC-specific IgM and IgG3 but reduced SRBC-specific IgG1 levels in Regnase-1$^{f/f}$ hCD20Tam^{Cre} mice (Fig. 6 E), indicating a suboptimal T cell–dependent response. Overall, we conclude that Regnase-1 plays a role in T cell–dependent antibody responses in B cells.

Regnase-1 contributes to maintenance of the GC reaction
After establishing a critical role for Regnase-1 in GC B cells and isotype switching, we sought to determine if the requirement for Regnase-1 for GC control continues once the class switching has initiated in an ongoing GC response. This enabled us to
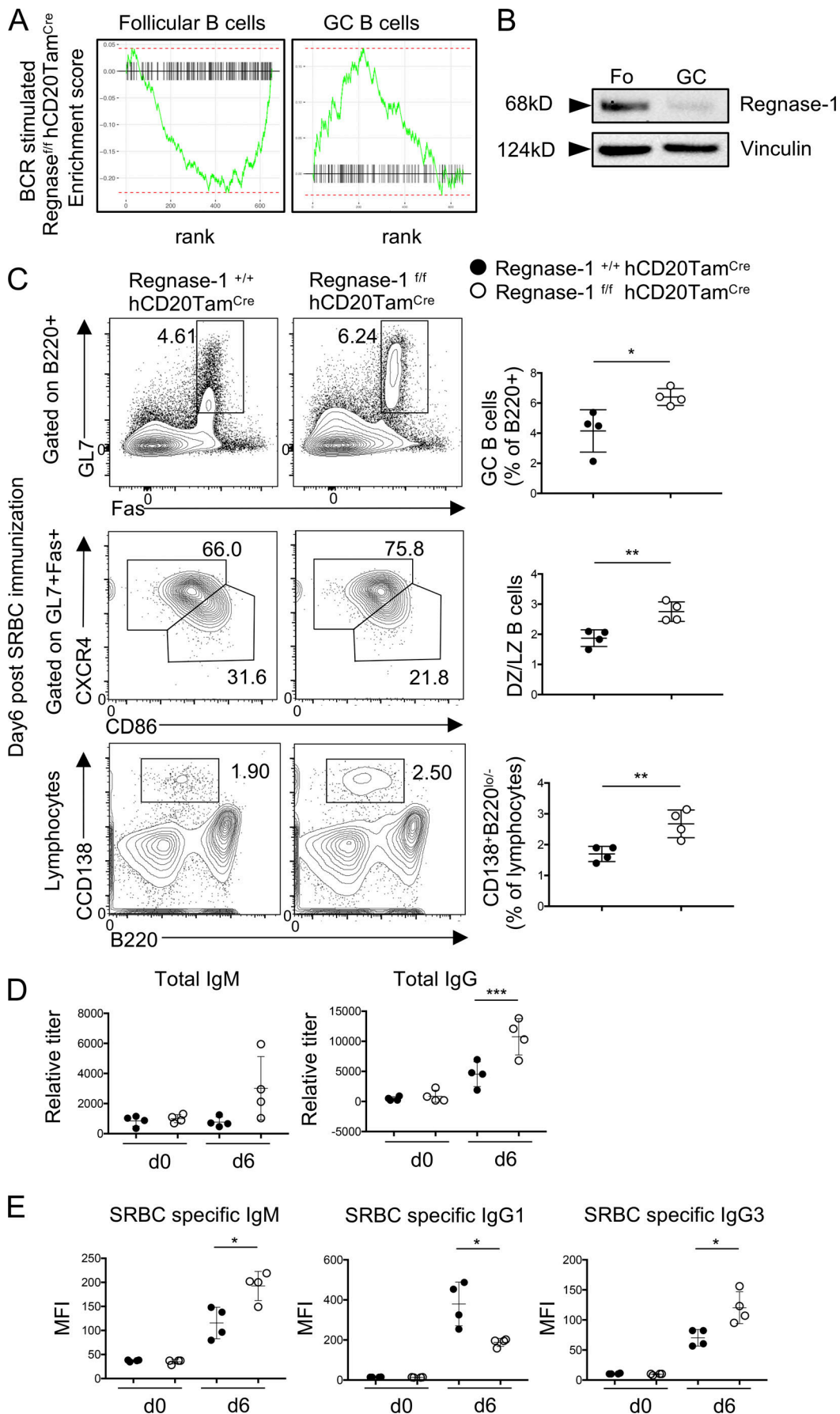
Figure 6. **Regnase-1 controls peripheral differentiation of B cells. (A)** GSEA of transcripts in BCR-stimulated, Regnase-1–deleted B cells. Significant enrichment of signatures associated with follicular and GC gene signatures; adjusted P values of 0.0869 and 0.00627, respectively, are shown. n = 3 or 4 animals; RNA-seq performed once. **(B)** Western blot showing Regnase-1 protein in follicular B (Fo) cells and GC B cells from spleens of mice immunized with SRBCs for 7 d (n = 2–3; three independent experiments). **(C)** Representative flow cytometry plots (left) and plotted frequencies (right) from spleens of mice of indicated genotypes analyzed day 6 after SRBC immunization and probed for GL7+ Fas+ cells (top), further subgated to probe for the surface expression of CXCR4 and CD86 (middle), and splenic lymphocytes probed for CD138+B220[lo or −] B cells (bottom). **(D)** Total IgM and IgG in the sera of immunized mice of indicated genotype, collected before and after 6 d of immunization, measured by sandwich ELISA. **(E)** SRBC binding IgM, IgG1, and IgG3 in the sera of immunized mice of indicated genotypes; plotted MFIs as measured by flow cytometry. **(C–E)** Each circle represents an animal; solid circles = Regnase-1+/+ hCD20Tam[Cre], clear circles = Regnase-1[f/f] hCD20Tam[Cre] (n = 3–5 mice; three independent experiments). Mice were administered three doses of tamoxifen i.p. on alternate days, immunized on day 7 after the first tamoxifen dose. Horizontal lines in the graphs indicate means with SD shown by error bars. Statistical significance calculated by unpaired Student's t test (*, P < 0.05; **, P < 0.01; ***, P < 0.001).

determine if Regnase-1–mediated control of peripheral differentiation of B cells is independent of its role in aberrant class switching of B cells. To address this question, we used a GC B cell–restricted deletion model by crossing Regnase-1[f/f] mice with Cγ1[Cre] mice, in which the Cre recombinase is induced upon initiation of IgG1 constant region (*Ighg1*) gene transcription (Casola et al., 2006). In this system, deletion of Regnase-1 would occur after antigenic stimulation and after the transcription of IgG1 locus has begun in B cells. Immunization of Regnase-1[f/f] Cγ1[Cre] mice with SRBCs did not result in a significant difference in their GC B cell frequencies compared with controls (Fig. 7 A). However, Regnase-1[f/f] Cγ1[Cre] mice showed a higher DZ/LZ B cell ratio compared with control mice (Fig. 7 A). In addition, antigen-specific antibody responses were higher in Regnase-1[f/f] Cγ1[Cre] mice with significantly elevated SRBC-specific IgG1 levels (Fig. 7 B).

Thus, in addition to its role in preventing aberrant GC formation (Fig. 6), Regnase-1 also contributes to the control of the antibody response and maintenance of the GC reaction and in zonal distribution of B cells in the GCs after antigenic stimulation.

Regnase-1 is required for preventing immunopathology throughout the course of B cell development

We observed striking immunopathology resulting from deletion of Regnase-1 during early B cell development. We next asked if Regnase-1 was required for controlling B cell–mediated immunopathology in late B cell maturation and differentiation. To address this hypothesis, Regnase-1[f/f] Cγ1[Cre] mice and the Regnase-1+/+ Cγ1[Cre] controls were maintained in a specific pathogen–free (SPF) animal facility for over a year, without external immunization but subjected to environmental antigens including those from commensal microbiota, to ensure a minimal basal level of antigenic challenge to the immune system of the mice. The mice were monitored over this time, and we found that Regnase-1[f/f] Cγ1[Cre] mice began to die at 10 mo of age and developed features similar to the diseased Regnase-1[f/f] Mb1[Cre] mice, including swollen abdomens and dermatitis. Sera were collected from these animals at regular intervals throughout the course of this experiment. Terminal phenotypic characterization of these animals revealed that two thirds of the mice developed severe immunopathology similar to the young Regnase-1[f/f] Mb1[Cre] mice, including enlarged secondary lymphoid organs (data not shown), disrupted architecture of lymphoid follicles, and immune cell infiltration in the liver (Fig. 8 A and Fig. 8 B). Splenocytes from Regnase-1[f/f] Cγ1[Cre] mice had a

higher frequency of B220[lo]CD138+ plasma cells than the controls (Fig. 8 C). In addition, the frequency class-switched IgG1+ B cells in these mice was also higher, which was not surprising given that the deletion of Regnase-1 in this model occurs in cells in which isotype class switching to IgG1 is already predetermined (Fig. 8 C). Sera from these mice collected serially over time showed a gradual increase in total IgG levels that was significantly higher than the controls at the terminal time point (Fig. 8 D). Overall, the aged Regnase-1[f/f] Cγ1[Cre] mice recapitulated the immunopathological phenotype observed upon early deletion of Regnase-1 in B cells (Regnase-1[f/f] Mb1[Cre]). However, the pathology among Regnase-1[f/f] Cγ1[Cre] mice was idiosyncratic in terms of severity, with only two thirds of the mice exhibiting severe disease. This was expected, as the immunological challenges that the mice were subjected to in the SPF facility were spontaneous and thus heterogenous. Thus, Regnase-1 prevents B cell–mediated immunopathology continuously throughout the course of B cell development and peripheral differentiation.

Discussion

This study demonstrates an essential and novel role for Regnase-1 in preventing B cell–dependent autoimmunity. Regnase-1 deletion in mice during early B cell development resulted in a severe immunopathological phenotype characterized by lymphoid hypertrophy, altered B cell subsets with increased activation marker expression, and elevated polyreactive serum antibodies (Fig. 1 and Fig. 2). The strong phenotype that we observed in young adult mice highlights the importance of B cell tolerance to avoid autoimmune and inflammatory disease outcomes. Although B cells have been implicated in the pathology of several autoimmune diseases, the evidence pointing to B cells as the cell type of origin in the pathophysiology is not ample (Franks et al., 2016). However, our findings are in line with several studies conducted in murine models showing that breach of tolerance mechanisms in B cells can cause autoimmune disease, as demonstrated by the phenotypes associated with B cell–specific deletion of *Fas*, *Ikzf1*, or *Lyn* in mice (Hao et al., 2008; Lamagna et al., 2014; Schwickert et al., 2019). Thus, our study provides further insights into B cells possibly having a causative role in morbid immunopathologies. Notably, the lethal autoimmune disease observed upon germline deletion of Regnase-1 has been mainly attributed to its T cell–specific role, as T cell deletion of Regnase-1 also results in severe inflammation leading to fatality in mice (Matsushita et al., 2009; Uehata
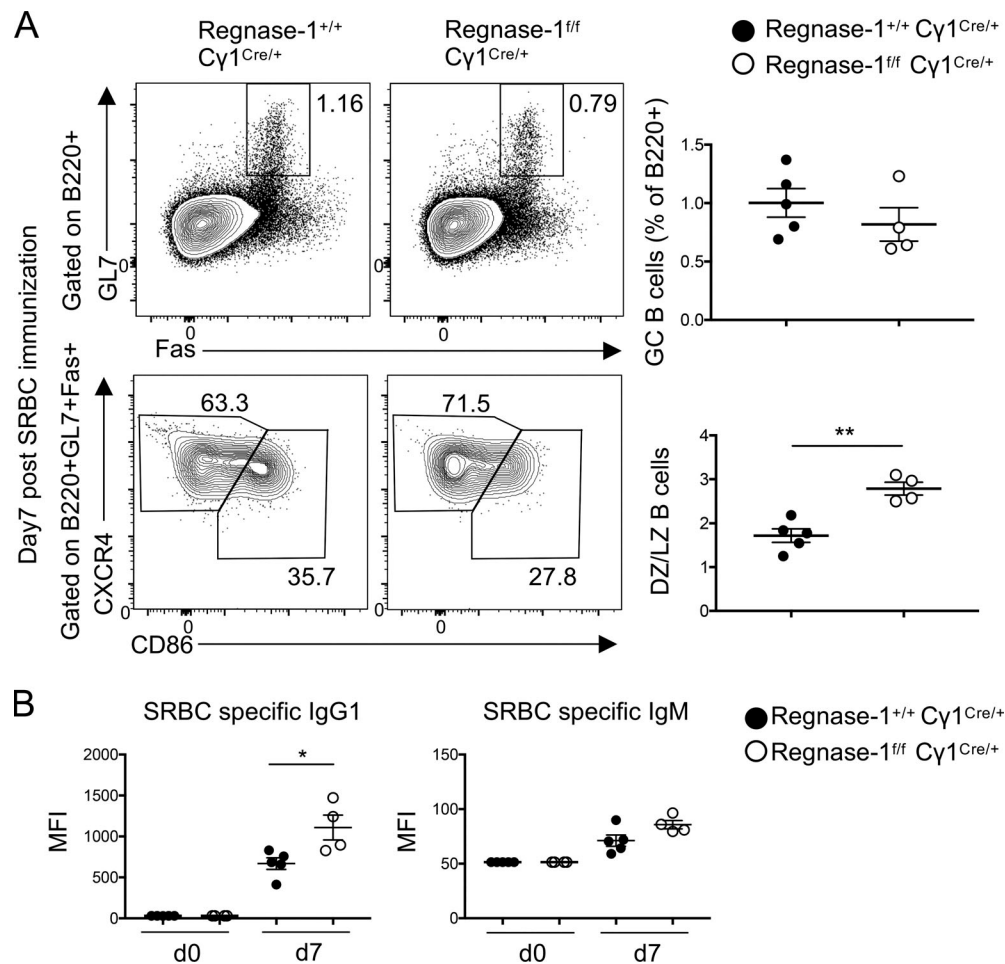
Figure 7. **Regnase-1 is critical for maintaining GCs. (A)** Representative flow cytometry plots (left) and plotted frequencies (right) from spleens of mice of indicated genotypes analyzed at day 7 after SRBC immunization and probed for GL7+ Fas+ cells (top), further subgated to probe for the surface expression of CXCR4 and CD86 (bottom). **(B)** SRBC binding IgG1 and IgM in the sera of immunized mice of indicated genotypes, plotted MFIs as measured by flow cytometry. **(A and B)** Each circle represents an animal; solid circles = Regnase-1+/+ Cγ1Cre/+, and clear circles = Regnase-1f/f Cγ1Cre/+ (n = 3–6 mice; three independent experiments). Horizontal lines in the graphs indicate means with SD shown by error bars. Statistical significance calculated by unpaired Student's t test (*, P < 0.05; **, P < 0.01).

et al., 2013). This observation has led to extensive studies in T cells in the past decade pertaining to the mechanism of Regnase-1–mediated immune regulation. Therefore, our study provides important new insights into the immunoregulatory functions of Regnase-1. We show that B cell growth and class switching were enhanced in the absence of Regnase-1 (Fig. 5). Inducible deletion in mature B cells also resulted in aberrant differentiation of B cells with an augmented GC and plasma cell response to immunization, showing that Regnase-1 controlled peripheral differentiation of B cells (Fig. 6). The requirement for Regnase-1 in controlling aberrant B cell responses continues throughout development and differentiation, even after B cells have been activated and have received costimulatory signals from T cells, as demonstrated by immunopathology and a dysregulated B cell response in a GC B cell–restricted deletion model of Regnase-1 (Fig. 7 and Fig. 8). Thus, our study highlights the importance of B cell responses in autoimmune diseases and also provides new insights into the molecular control of Regnase-1 in the regulation of such responses.

RNA-seq analysis revealed that Regnase-1 controlled molecular pathways in B cells that enhance survival and proliferation, BCR signaling, interleukin and growth factor regulation G1-S transition of the cell cycle, and pathways that regulate the GC reaction (Fig. 3, Fig. 4, and Fig. 6 A). B cell–specific transcripts that were up-regulated upon Regnase-1 deletion, such as *Tnfrsf13b* and *Bcl2*, promote survival of antibody-secreting cells, and *Tnfrsf13b* and *Batf* are crucial for isotype class switching. Up-regulation of these transcripts and the molecular pathways and differentiation networks associated with Regnase-1 loss were consistent with the altered B cell responses that we observed in the Regnase-1 mouse models used in this study, which showed increased class switching and plasma cell frequency upon ex vivo stimulation of naive B cells, as well as during immunizations in mice (Fig. 5 and Fig. 6). Interestingly, a recent study of tumor-infiltrating T cells also showed a critical role of Regnase-1 in regulating the persistence of effector T cells that was mediated by *Batf* (Wei et al., 2019). While our data indicated that Batf mRNA is possibly posttranscriptionally regulated by
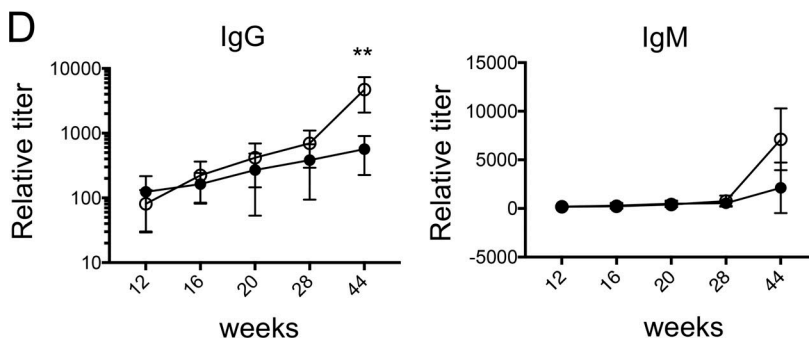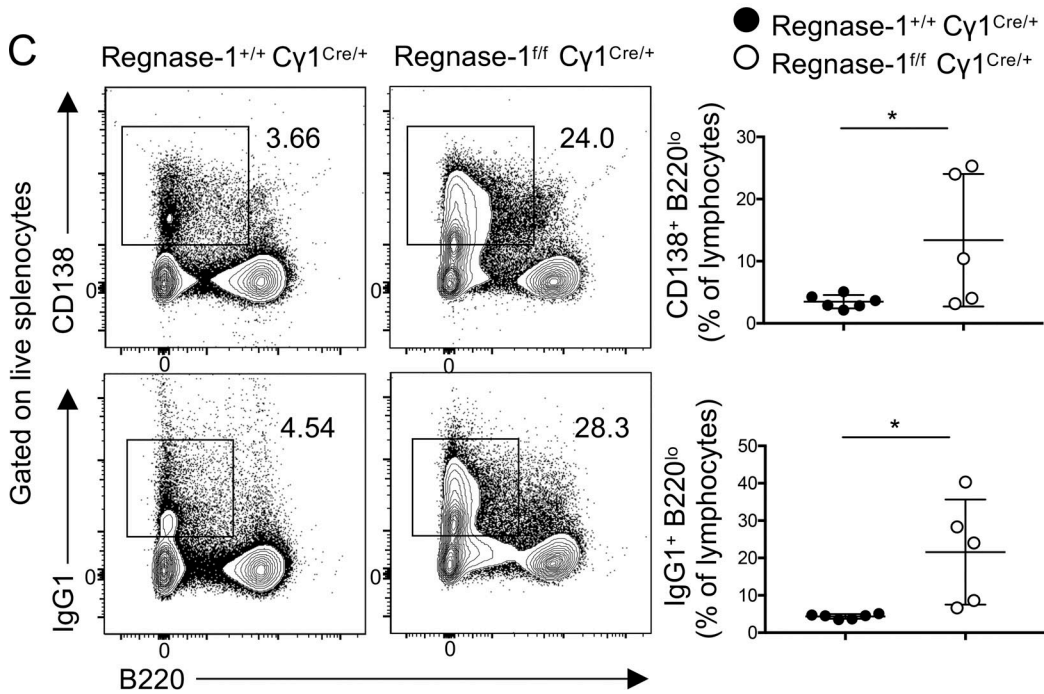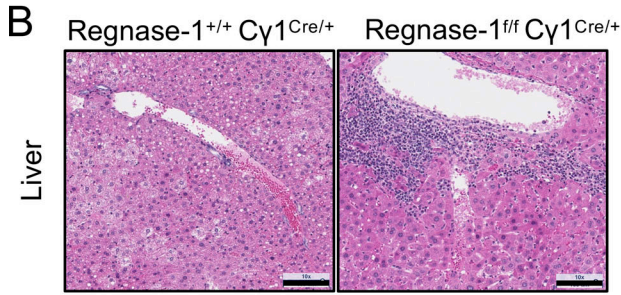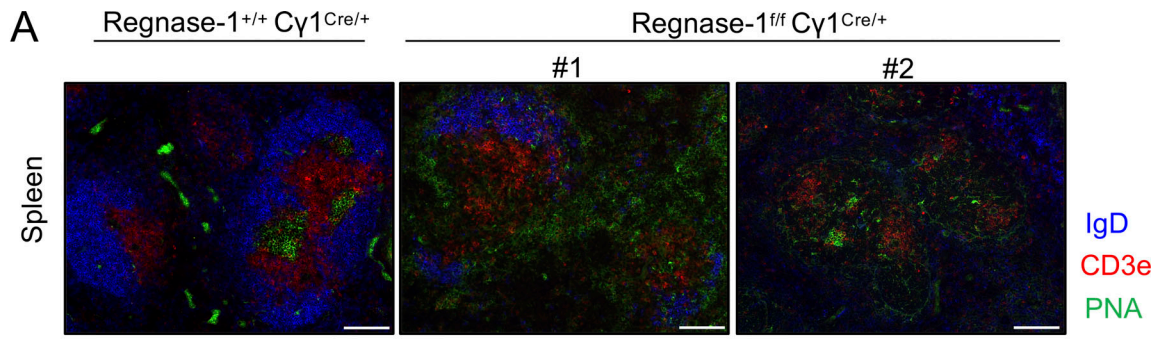
A

Regnase-1$^{+/+}$ Cγ1$^{Cre/+}$

Regnase-1$^{f/f}$ Cγ1$^{Cre/+}$

#1 #2

Spleen

IgD
CD3e
PNA

B

Regnase-1$^{+/+}$ Cγ1$^{Cre/+}$ Regnase-1$^{f/f}$ Cγ1$^{Cre/+}$

Liver

C

● Regnase-1$^{+/+}$ Cγ1$^{Cre/+}$
○ Regnase-1$^{f/f}$ Cγ1$^{Cre/+}$

Regnase-1$^{+/+}$ Cγ1$^{Cre/+}$ Regnase-1$^{f/f}$ Cγ1$^{Cre/+}$

Gated on live splenocytes

CD138

3.66

24.0

CD138$^+$ B220^{lo} (% of lymphocytes)

*

IgG1

4.54

28.3

IgG1$^+$ B220^{lo} (% of lymphocytes)

*

B220

D

IgG

Relative titer

**

12 16 20 28 44

weeks

IgM

Relative titer

12 16 20 28 44

weeks

Bhat et al.
Role of Regnase-1 in B cells

Journal of Experimental Medicine   13 of 18
https://doi.org/10.1084/jem.20200971

Figure 8. **Regnase-1 controls immunopathology after B cell differentiation. (A)** Representative immunofluorescence images of spleens from 44-wk-old mice of indicated genotypes, Regnase-1$^{f/f}$ Cγ1$^{Cre/+}$ mice with less severe disease (middle), Regnase-1$^{f/f}$ Cγ1$^{Cre/+}$ mice with more severe disease (right). Cryosections stained for follicular B cells (IgD in blue), GC B cells (PNA in green), and T (CD3e in red). Scale bars = 100 μM (n = 2 or 3 mice; two independent experiments). **(B)** H&E staining of livers collected from 44-wk-old mice of indicated genotypes. Scale bars = 100 μM (n = 3 mice; two independent experiments). **(C)** Representative flow cytometry plots (left) and plotted frequencies (right) from spleens of mice of indicated genotypes analyzed at 44 wk of age, splenic lymphocytes probed for CD138$^+$B220$^-$ B cells (top), and for IgG1$^+$B220$^-$ B cells. Each circle represents an animal, solid circles = Regnase-1$^{+/+}$ Cγ1$^{Cre/+}$, clear circles = Regnase-1$^{f/f}$ Cγ1$^{Cre/+}$. **(D)** Mean and standard deviation of relative titers of total IgM and IgG in the sera collected at the indicated time points from mice of indicated genotype (n = 5 or 6), measured by sandwich ELISA. **(C and D)** n = 4–6 mice; two independent experiments. Horizontal lines in the graphs indicate means with SD shown by error bars. Statistical significance calculated by unpaired Student's t test (*, P < 0.05; **, P < 0.01).

Regnase-1 in B cells (Fig. S3 C), the study by Wei et al. (2019) found *Batf* to be a direct substrate of Regnase-1, with a role in promoting metabolic fitness of T cells. This not only validates our findings but also highlights the context-specificity of Regnase-1 and its targets, given that BATF is essential for, and promotes, AID expression in B cells, but its Regnase-1–associated function in effector T cells during anti-tumor activity is mediated by increased metabolic fitness.

The pathological features observed upon B cell–specific ablation of Regnase-1 appear to stem from an aberrant GC reaction. GC B cell differentiation, antibody response, and the ratio of DZ to LZ B cell frequency was enhanced in mice bearing Regnase-1–deficient B cells (Fig. 6 and Fig. 7). This may have resulted from an expanded DZ or a diminished LZ compartment. Such skewed GC response might cause a high rate of somatic hypermutation in the absence of Regnase-1 but impaired affinity-based selection of B cells, therefore predicting a suboptimal response to commensal and pathogenic antigens. While these possibilities warrant further investigation, they suggest a potentially critical role of Regnase-1 in fine-tuning the adaptive immune responses to pathogens and other antigenic challenges. Therefore, it is pertinent that the role of Regnase-1 is explored in the context of viral and other microbial infections. An interesting finding from our study was that the antibody response and zonal distribution of B cells were altered in immunized Regnase-1$^{f/f}$ Cγ1^{Cre} mice (Fig. 7). This was unexpected, as we found Regnase-1 protein to be strongly down-regulated in GC B cells (Fig. 6 B). Therefore, deletion of Regnase-1 after GC formation should have hypothetically not resulted in an alteration in further differentiation of B cells. However, we reasoned that since the low Regnase-1 protein levels in GC B cells were observed using bulk analysis, we may need to study Regnase-1 expression in GC B cells at a higher resolution. In addition, we have previously shown that MALT1 proteolytic activity is localized in GC B cells and is restricted within foci or clusters of B cells (Lee et al., 2017), which makes it likely that Regnase-1 protein turnover is regulated within the GC B cells in a dynamic and heterogeneous fashion. This is particularly important in the context of interzonal cycling of B cells within GCs, which is known to be stringently regulated by surges in expression levels of transcription factors and regulatory genes that punctuate these transitions to ensure appropriate selection (Dominguez-Sola et al., 2015; Dominguez-Sola et al., 2012; Sander et al., 2015; Victora et al., 2010). One of the possible mechanisms of the dynamic regulation of GC B cells by Regnase-1 could be mediated by its transient expression in a small subset of LZ B cells initiating their transition to the DZ

phase, akin to c-Myc regulation of cell cycle entry and interzonal migration of GC B cells (Dominguez-Sola et al., 2012). Such a role of Regnase-1 would reconcile the lack of Regnase-1 protein observed in the GC B cell lysates and the GC-associated phenotype observed upon Cγ1^{Cre}-mediated deletion of Regnase-1 (Fig. 6 B, Fig. 7, and Fig. 8). However, delving further into the dynamic regulatory mechanisms of Regnase-1 would require tracking B cells in the GC at a single-cell level.

Overall, we demonstrate that B cell–specific deletion of Regnase-1 resulted in perturbations in B cell responses in all the mouse models tested in this study. However, it remains to be determined whether the observed pathologies in these models are driven in a B cell–intrinsic fashion or are a cumulative outcome of interaction and cross-activation of multiple components of the immune system, such as possible aberrant T cell recruitment by Regnase-1–deficient B cells. This would warrant further investigation and would be critical for a thorough understanding of the pathogenesis of B cell–driven immune system diseases. Moreover, it must be noted that minor leakiness reported in the Mb1 (*Cd79a*) Cre–driven recombination could potentially have some confounding effect on the phenotype observed (Hobeika et al., 2006). However, recombination in hCD20Tam^{Cre} and Cγ1^{Cre} is highly specific to B cells, thus ascertaining that B cell deletion of Regnase-1 is the original source of phenotypic characteristics observed in these mice. To further understand the molecular underpinnings of Regnase-1–mediated regulation of B cells, it will be critical to determine which of the potential targets identified from the RNA-seq analysis in this study are consequential for B cell regulation and their mode of regulation. In addition, the role of Regnase-1 in BCR signal transduction in the context of MALT1 function in B cells remains to be determined.

Our findings and the previously published studies showing Regnase-1–mediated regulation of T cells and tumor-infiltrating T cells in solid cancers (Uehata et al., 2013; Wei et al., 2019) and the association of Regnase-1 mutations with diffuse large B cell lymphoma (Schmitz et al., 2018) offer potential for Regnase-1 to be explored as a therapeutic target. However, further understanding of immune regulation by Regnase-1 would be critical for harnessing the therapeutic potential of Regnase-1 in the context of autoimmunity and cancers. In cancers, with the exception of lymphomas associated with Regnase-1 loss of function, suppressing Regnase-1 could possibly have positive outcomes, particularly in the form of cell-based immunotherapy, whereas enhancing Regnase-1 activity may ameliorate autoimmune and inflammatory diseases. However, the potential

for Regnase-1 targeting as cancer immunotherapy such as that described by Wei et al. (2019) will need to be cell type specific, and any therapeutic approach targeting Regnase-1 needs to approached with caution, as complete inhibition or overactivity of Regnase-1 may have deleterious immunopathological outcomes. Thus, seeking therapeutic strategies that have modulatory action on Regnase-1 could yield more favorable outcomes for both autoimmune disease and cancer.

Materials and methods

Mice
Regnase-1[f/f] mice were generated as described (Li et al., 2017). These mice were crossed with either Mb1[Cre], hCD20Tam[Cre], or Cγ1[Cre] mice (Casola et al., 2006; Hobeika et al., 2006; Khalil et al., 2012). Cre activation in Regnase-1[f/f] hCD20Tam[Cre] and Regnase-1^{+/+} hCD20Tam[Cre] (controls) was induced with intraperitoneal injections on 5 consecutive d or 3 alternate d (indicated in the respective figure legends) with 1 mg tamoxifen (Sigma) in a 10% (vol/vol) ethanol-in–olive oil solution.

B cells were isolated from tamoxifen-treated mice for ex vivo studies, including Ca^{2+} flux, proliferation, immunoblots, in vitro stimulation, and RNA-seq, at day 11 after first tamoxifen dose. Immunizations with SRBCs were done at day 7 after first tamoxifen dose, and the animals were sacrificed on the time points indicated in the respective figure legends. Experimental animals (combination of male or female mice) were age matched for all experiments. Animals were bred and housed at the SPF facility at the Sanford Burnham Prebys Medical Discovery Institute (SBP), and the Institutional Animal Care and User Committee guidelines were followed while carrying out all animal experiments.

Histology
Tissues were frozen in Tissue-TEK OCT (Sakura Finetek) compound at –80°C. For immunofluorescent staining, 6-μM sections were mounted on Superfrost Plus slides (Thermo Fisher Scientific), fixed with cold acetone for 10 min, and blocked with 5% FBS. The following antibodies were used to stain the sections: peanut agglutinin (Vector Labs) and B220 (RA3-6B2; Thermo Fisher Scientific) for 2 h at room temperature and washed with a 0.5% Tween in PBS (vol/vol) solution. Images were acquired using a Zeiss Axio ImagerM1 microscope and Slidebook software (Intelligent Imaging Innovations).

For H&E staining, tissues were fixed in 10% zinc formalin, and staining and scanning were performed by the SBP histology core facility.

Immunizations
Animals were immunized with intraperitoneal injections with 100 μl citrated SRBCs (Colorado Serum Company) that were washed twice with PBS and resuspended at 10% (vol/vol) in PBS. Sera for measuring antibodies were collected on day 0 and day 6 or 7 of injections.

Serum antibody assays
Total serum Ig was measured by sandwich ELISA. High-binding assay plates were coated overnight with 50 μl capture antibody (Bethyl Labs) diluted in carbonate buffer. Plates were washed with wash buffer (0.1% Tween20 in PBS) and blocked for 2 h at 37°C with 50 μl of 5% BSA and 0.05% sodium azide in PBS. After washing, 50-μl mouse serum samples (diluted in 1% BSA and 0.1% Tween20 in PBS) were added and incubated for 2 h at 37°C. Plates were washed and incubated with alkaline phosphatase–conjugated detection antibodies (Bethyl Labs) for 1 h. Plates were washed and incubated with 100 μl phosphatase substrate solution (Sigma) for 10–15 min, and absorbance was measured at 405 nm.

Polyreactivity was assessed by performing ELISA as previously described (Gitlin et al., 2016) using cardiolipin (Sigma), LPS (Sigma), human insulin (Sigma), double-stranded DNA (Sigma), and KLH (Sigma).

SRBC-specific IgM, IgG3, and IgG1 in the sera were measured by flow cytometry–based MFIs (median fluorescence intensity) of anti-IgM (Clone II/41; eBioscience), anti-IgG3 (Clone R40-82; BD PharMingen), and anti-IgG1 (A85-1; BD Biosciences) binding to SRBC-bound serum antibodies using a method described previously (McAllister et al., 2017).

Western blots
Freshly isolated splenocytes were enriched for B cells using CD43 magnetic bead–based depletion and stimulated in RPMI 1640 with or without stimuli. Cells were collected at various time points and lysed with 1% SDS. Lysates were run on 4–12% gradient polyacrylamide Bis-Tris gels (Invitrogen). The resolved proteins were transferred to polyvinylidene difluoride membranes using the BOLT transfer system (Thermo Fisher Scientific). The following antibodies were used to probe for various proteins: Regnase-1 (GeneTex), Bcl2 (BD Biosciences), Vinculin (Cell Signaling Technology), and b-Actin (Cell Signaling Technology).

For the immunoblots with GC B cells and follicular B cells (Fig. 6 B), wild-type mice were immunized with SRBCs, and GC and follicular B cells isolated by magnetic bead–based depletion using the strategy previously described (Cato et al., 2011).

Flow cytometry
Single-cell suspensions of spleens were subjected to RBC lysis with ACK buffer and stained in FACS buffer (1% FBS and 0.05% sodium azide in PBS).

Surface staining of cell suspensions was performed by treating the cells with anti-CD16/32 (clone 24G2; BD Biosciences), followed by staining with these antibodies: B220 (RA3-6B2), IgM (II/41), Fas (Jo2), GL7, CXCR4 (L276F12), IgG1 (A85-1), IgG3 (R40-82), CD86 (GL-1), CD138 (281–2), CD11c (N418), and T-bet (4B10). The flow cytometry assays were run on FACS Canto (BD Biosciences), and analysis was performed using FlowJo (Treestar) software.

Calcium flux assay was performed by measuring the ratio of bound to unbound calcium indicator Indo-1 AM, which was loaded into splenic B cells that were either left untreated or were treated with probenecid (Thermo Fisher Scientific) before acquisition. After acquisition of baseline for 20 s, cells were treated with the indicated stimuli, and data were acquired on LSR Fortessa X-20 (BD Biosciences) and analyzed using FlowJo (Treestar) software.

In vitro stimulation of naive splenic B cells

Splenic B cells were isolated by magnetic bead–based depletion using CD43 Microbeads (Miltenyi) after ACK buffer treatment to lyse RBCs. Cells were left either unstimulated or stimulated with the indicated combinations of 10 µg/ml anti-IgM (Jackson ImmunoResearch), 5 µg/ml anti-CD40 (1C10; Thermo Fisher Scientific), 10 ng/ml rIL4 (Thermo Fisher Scientific), and 10 µg/ml LPS (InvivoGen). For the in vitro proliferation assay, the cells were loaded with eFluor 670 dye (eBioscience) and cultured for 3 d in RPMI 1640 (Corning) supplemented with 10% FBS (Sigma), penicillin-streptomycin, MEM Nonessential Amino Acids (Corning), 1 mM sodium pyruvate, 2 mM GlutaMax, and 55 µM 2-mercaptoethanol (Thermo Fisher Scientific). Proliferation was assessed by determining dilution of the dye by flow cytometry.

RNA-seq

Transcriptome analysis was performed on 13 RNA samples, which comprised four control samples from naive B cells (Regnase-1$^{+/+}$ hCD20Tam^{Cre}), three samples each from Regnase-1–deficient naive B cells (Regnase-1$^{f/f}$ hCD20Tam^{Cre}), BCR-stimulated control B cells (BCR–Regnase-1$^{+/+}$ hCD20Tam^{Cre}), and Regnase-1–deficient BCR-stimulated B cells (BCR–Regnase-1$^{f/f}$ hCD20Tam^{Cre}). Splenic B cells were isolated by negative selection with CD43 beads (Miltenyi). BCR stimulation was done for 4 h with 10 µg/ml of anti-IgM F(ab′)2 (Jackson ImmunoResearch) in RPMI 1640 medium (Corning). Cells were lysed with the TRIzol reagent (Invitrogen), and RNA was isolated using chloroform and isopropanol. RNA was washed with ethanol and passed through the Qiagen RNA cleanup kit for further purification. RNA-seq was done at the La Jolla Institute for Immunology sequencing core facility using Hiseq2500 technology from Illumina with single-end 50-bp reads. Pathway analysis was performed using the Metacore platform. For GSEA methods, the fgsea package was used, and analysis was performed with minSize = 1, maxSize = 500, and 100,000 permutations. A Benjamini-Hochberg–adjusted P value of 0.1 was used for significance.

Genes that were differentially expressed in the Regnase-1$^{f/f}$ hCD20Tam^{Cre} versus controls were uploaded to GeneGo, and enrichment analysis was performed. Both up and down signals were selected using a threshold = 0; P value = 0.1.

The DESeq2 package was used for differential expression analysis using the following model: Stimulation + Genotype + Stimulation:Genotype. A Benjamini-Hochberg–adjusted P value of 0.1 was used as the threshold for significance. For GSEA, BCR stimulation–dependent genes that were regulated by Regnase-1 were identified using an alternative model: Stimulation + Stimulation:Genotype.

RT-qPCR

cDNA was prepared from 100 ng RNA per sample with iScript Reverse Transcription Supermix (Bio-Rad) using the manufacturer's protocol. RT-qPCR was performed using SYBR Green Supermix (Bio-Rad). The following primer sequences were obtained from PrimerBank (Spandidos et al., 2010) for the following genes: *Batf* (forward) 5′-CACAGAAAGCCGACACCCTT-3′, *Batf* (reverse) 5′-GCTGTTTGATCTCTTTGCGGA-3′; *Tnfrsf13b* (forward) 5′-GAGCAAGGCAGGTACTACGAC-3′, *Tnfrsf13b* (reverse) 5′-TCGCTACTTAGCCTCAATCCT-3′; *Bcl2* (forward) 5′-ATGCCTTTGTGGAACTATATGGC-3′, *Bcl2* (reverse) 5′-GGTATGCACCCAGAGTGATGC-3′; and *GAPDH* (forward) 5′-CATGGCCTTCCGTGTTCCTA-3′, *GAPDH* (reverse) 5′-CCTGCTTCACCACCTTCTTGAT-3′. The mRNA level of each tested gene was normalized to *GAPDH*, and fold change was calculated by the ΔΔCt method.

Statistical analysis

GraphPad Prism software and R were used for statistical analysis. Statistically significant differences in experimental readouts are indicated by asterisks. Tests performed to determine statistical significance are indicated in the respective figure legends.

Data availability

Data from RNA-seq have been deposited in the Gene Expression Omnibus repository and are available under accession no. GSE147799.

Online supplemental material

Fig. S1 shows immunopathological features by H&E staining of inguinal lymph node sections and immunofluorescent images of kidney sections of Regnase-1$^{f/f}$ Mb1^{Cre} mice and Regnase-1$^{+/+}$ Mb1^{Cre} control mice. Fig. S2 shows phenotypic analysis of altered B cell populations in Regnase-1$^{f/f}$ Mb1^{Cre} mice including CD11c$^+$ B cells and splenic and peritoneal B1 B cells and altered expression of surface markers such as CD43, CD21, and CD23 in splenic B cells. Fig. S3 shows a schematic of tamoxifen administration to Regnase-1$^{f/f}$ hCD20Tam^{Cre} mice and Regnase-1$^{+/+}$ hCD20Tam^{Cre} control mice, immunoblots showing deletion of Regnase-1, and posttranscriptional regulation of select targets from the RNA-seq analysis of Regnase-1–deficient cells. Fig. S4 shows Regnase-1 expression in B cells in the absence of MALT1, Ca2$^+$ flux upon BCR activation in Regnase-1–deficient B cells, and heatmaps indicating gene signatures of follicular and GC B cells that are differentially expressed in the absence of Regnase-1 in B cells. Table S1 includes pathway and gene network analysis from the Metacore platform generated from the RNA-seq of Regnase-1–deficient B cells.

References

Arkatkar, T., H.M. Jacobs, S.W. Du, Q.Z. Li, K.L. Hudkins, C.E. Alpers, D.J. Rawlings, and S.W. Jackson. 2018. TACI deletion protects against progressive murine lupus nephritis induced by BAFF overexpression. *Kidney Int.* 94:728–740. https://doi.org/10.1016/j.kint.2018.03.012

Behrens, G., R. Winzen, N. Rehage, A. Dörrie, M. Barsch, A. Hoffmann, J. Hackermüller, C. Tiedje, V. Heissmeyer, and H. Holtmann. 2018. A translational silencing function of MCPIP1/Regnase-1 specified by the target site context. *Nucleic Acids Res.* 46:4256–4270. https://doi.org/10.1093/nar/gky106

Betz, B.C., K.L. Jordan-Williams, C. Wang, S.G. Kang, J. Liao, M.R. Logan, C.H. Kim, and E.J. Taparowsky. 2010. Batf coordinates multiple aspects of B and T cell function required for normal antibody responses. *J. Exp. Med.* 207:933–942. https://doi.org/10.1084/jem.20091548

Bornancin, F., F. Renner, R. Touil, H. Sic, Y. Kolb, I. Touil-Allaoui, J.S. Rush, P.A. Smith, M. Bigaud, U. Junker-Walker, et al. 2015. Deficiency of MALT1 paracaspase activity results in unbalanced regulatory and effector T and B cell responses leading to multiorgan inflammation. *J. Immunol.* 194:3723–3734. https://doi.org/10.4049/jimmunol.1402254

Casola, S., G. Cattoretti, N. Uyttersprot, S.B. Koralov, J. Seagal, Z. Hao, A. Waisman, A. Egert, D. Ghitza, and K. Rajewsky. 2006. Tracking germinal center B cells expressing germ-line immunoglobulin γ1 transcripts by conditional gene targeting. *Proc. Natl. Acad. Sci. USA.* 103:7396–7401. https://doi.org/10.1073/pnas.0602353103

Castigli, E., S.A. Wilson, S. Scott, F. Dedeoglu, S. Xu, K.P. Lam, R.J. Bram, H. Jabara, and R.S. Geha. 2005. TACI and BAFF-R mediate isotype switching in B cells. *J. Exp. Med.* 201:35–39. https://doi.org/10.1084/jem.20032000

Cato, M.H., I.W. Yau, and R.C. Rickert. 2011. Magnetic-based purification of untouched mouse germinal center B cells for ex vivo manipulation and biochemical analysis. *Nat. Protoc.* 6:953–960. https://doi.org/10.1038/nprot.2011.344

Dominguez-Sola, D., G.D. Victora, C.Y. Ying, R.T. Phan, M. Saito, M.C. Nussenzweig, and R. Dalla-Favera. 2012. The proto-oncogene MYC is required for selection in the germinal center and cyclic reentry. *Nat. Immunol.* 13:1083–1091. https://doi.org/10.1038/ni.2428

Dominguez-Sola, D., J. Kung, A.B. Holmes, V.A. Wells, T. Mo, K. Basso, and R. Dalla-Favera. 2015. The FOXO1 Transcription Factor Instructs the Germinal Center Dark Zone Program. *Immunity.* 43:1064–1074. https://doi.org/10.1016/j.immuni.2015.10.015

Figgett, W.A., D. Deliyanti, K.A. Fairfax, P.S. Quah, J.L. Wilkinson-Berka, and F. Mackay. 2015. Deleting the BAFF receptor TACI protects against systemic lupus erythematosus without extensive reduction of B cell numbers. *J. Autoimmun.* 61:9–16. https://doi.org/10.1016/j.jaut.2015.04.007

Franks, S.E., A. Getahun, P.M. Hogarth, and J.C. Cambier. 2016. Targeting B cells in treatment of autoimmunity. *Curr. Opin. Immunol.* 43:39–45. https://doi.org/10.1016/j.coi.2016.09.003

Gitlin, A.D., L. von Boehmer, A. Gazumyan, Z. Shulman, T.Y. Oliveira, and M.C. Nussenzweig. 2016. Independent Roles of Switching and Hypermutation in the Development and Persistence of B Lymphocyte Memory. *Immunity.* 44:769–781. https://doi.org/10.1016/j.immuni.2016.01.011

Hao, Z., G.S. Duncan, J. Seagal, Y.W. Su, C. Hong, J. Haight, N.J. Chen, A. Elia, A. Wakeham, W.Y. Li, et al. 2008. Fas receptor expression in germinal-center B cells is essential for T and B lymphocyte homeostasis. *Immunity.* 29:615–627. https://doi.org/10.1016/j.immuni.2008.07.016

Hao, Y., P. O'Neill, M.S. Naradikian, J.L. Scholz, and M.P. Cancro. 2011. A B-cell subset uniquely responsive to innate stimuli accumulates in aged mice. *Blood.* 118:1294–1304. https://doi.org/10.1182/blood-2011-01-330530

He, B., W. Xu, P.A. Santini, A.D. Polydorides, A. Chiu, J. Estrella, M. Shan, A. Chadburn, V. Villanacci, A. Plebani, et al. 2007. Intestinal bacteria trigger T cell-independent immunoglobulin A(2) class switching by inducing epithelial-cell secretion of the cytokine APRIL. *Immunity.* 26:812–826. https://doi.org/10.1016/j.immuni.2007.04.014

Hobeika, E., S. Thiemann, B. Storch, H. Jumaa, P.J. Nielsen, R. Pelanda, and M. Reth. 2006. Testing gene function early in the B cell lineage in mb1-cre mice. *Proc. Natl. Acad. Sci. USA.* 103:13789–13794. https://doi.org/10.1073/pnas.0605944103

Holmdahl, R., F. Nimmerjahn, and R.J. Ludwig. 2019. Editorial: Autoantibodies. *Front. Immunol.* 10:484. https://doi.org/10.3389/fimmu.2019.00484

Inoue, T., R. Shinnakasu, W. Ise, C. Kawai, T. Egawa, and T. Kurosaki. 2017. The transcription factor Foxo1 controls germinal center B cell proliferation in response to T cell help. *J. Exp. Med.* 214:1181–1198. https://doi.org/10.1084/jem.20161263

Ise, W., M. Kohyama, B.U. Schraml, T. Zhang, B. Schwer, U. Basu, F.W. Alt, J. Tang, E.M. Oltz, T.L. Murphy, and K.M. Murphy. 2011. The transcription factor BATF controls the global regulators of class-switch recombination in both B cells and T cells. *Nat. Immunol.* 12:536–543. https://doi.org/10.1038/ni.2037

Jeltsch, K.M., and V. Heissmeyer. 2016. Regulation of T cell signaling and autoimmunity by RNA-binding proteins. *Curr. Opin. Immunol.* 39:127–135. https://doi.org/10.1016/j.coi.2016.01.011

Kafasla, P., A. Skliris, and D.L. Kontoyiannis. 2014. Post-transcriptional coordination of immunological responses by RNA-binding proteins. *Nat. Immunol.* 15:492–502. https://doi.org/10.1038/ni.2884

Kaileh, M., and R. Sen. 2012. NF-κB function in B lymphocytes. *Immunol. Rev.* 246:254–271. https://doi.org/10.1111/j.1600-065X.2012.01106.x

Khalil, A.M., J.C. Cambier, and M.J. Shlomchik. 2012. B cell receptor signal transduction in the GC is short-circuited by high phosphatase activity. *Science.* 336:1178–1181. https://doi.org/10.1126/science.1213368

Kita, H., I.R. Mackay, J. Van De Water, and M.E. Gershwin. 2001. The lymphoid liver: considerations on pathways to autoimmune injury. *Gastroenterology.* 120:1485–1501. https://doi.org/10.1053/gast.2001.22441

Konieczny, P., A. Lichawska-Cieslar, P. Kwiecinska, J. Cichy, R. Pietrzycka, W. Szukala, W. Declercq, M. Devos, A. Paziewska, I. Rumienczyk, et al. 2019. Keratinocyte-specific ablation of Mcpip1 impairs skin integrity and promotes local and systemic inflammation. *J. Mol. Med. (Berl.).* 97:1669–1684. https://doi.org/10.1007/s00109-019-01853-2

Lamagna, C., Y. Hu, A.L. DeFranco, and C.A. Lowell. 2014. B cell-specific loss of Lyn kinase leads to autoimmunity. *J. Immunol.* 192:919–928. https://doi.org/10.4049/jimmunol.1301979

Lee, P., Z. Zhu, J. Hachmann, T. Nojima, D. Kitamura, G. Salvesen, and R.C. Rickert. 2017. Differing Requirements for MALT1 Function in Peripheral B Cell Survival and Differentiation. *J. Immunol.* 198:1066–1080. https://doi.org/10.4049/jimmunol.1502518

Li, Y., X. Huang, S. Huang, H. He, T. Lei, F. Saaoud, X.Q. Yu, A. Melnick, A. Kumar, C.J. Papasian, et al. 2017. Central role of myeloid MCPIP1 in protecting against LPS-induced inflammation and lung injury. *Signal Transduct. Target. Ther.* 2:17066. https://doi.org/10.1038/sigtrans.2017.66

Lucas, P.C., M. Yonezumi, N. Inohara, L.M. McAllister-Lucas, M.E. Abazeed, F.F. Chen, S. Yamaoka, M. Seto, and G. Nunez. 2001. Bcl10 and MALT1, independent targets of chromosomal translocation in malt lymphoma, cooperate in a novel NF-kappa B signaling pathway. *J. Biol. Chem.* 276:19012–19019. https://doi.org/10.1074/jbc.M009984200

Mackay, F., and P. Schneider. 2009. Cracking the BAFF code. *Nat. Immunol.* 9:491–502. https://doi.org/10.1038/nri2572

Matsushita, K., O. Takeuchi, D.M. Standley, Y. Kumagai, T. Kawagoe, T. Miyake, T. Satoh, H. Kato, T. Tsujimura, H. Nakamura, and S. Akira. 2009. Zc3h12a is an RNase essential for controlling immune responses by regulating mRNA decay. *Nature.* 458:1185–1190. https://doi.org/10.1038/nature07924

McAllister, E.J., J.R. Apgar, C.R. Leung, R.C. Rickert, and J. Jellusova. 2017. New Methods To Analyze B Cell Immune Responses to Thymus-Dependent Antigen Sheep Red Blood Cells. *J. Immunol.* 199:2998–3003. https://doi.org/10.4049/jimmunol.1700454

Mesin, L., J. Ersching, and G.D. Victora. 2016. Germinal Center B Cell Dynamics. *Immunity.* 45:471–482. https://doi.org/10.1016/j.immuni.2016.09.001

Minagawa, K., K. Wakahashi, H. Kawano, S. Nishikawa, C. Fukui, Y. Kawano, N. Asada, M. Sato, A. Sada, Y. Katayama, and T. Matsui. 2014. Post-transcriptional modulation of cytokine production in T cells for the regulation of excessive inflammation by TFL. *J. Immunol.* 192:1512–1524. https://doi.org/10.4049/jimmunol.1301619

Nemazee, D. 2017. Mechanisms of central tolerance for B cells. *Nat. Rev. Immunol.* 17:281–294. https://doi.org/10.1038/nri.2017.19

Nutt, S.L., N. Taubenheim, J. Hasbold, L.M. Corcoran, and P.D. Hodgkin. 2011. The genetic network controlling plasma cell differentiation. *Semin. Immunol.* 23:341–349. https://doi.org/10.1016/j.smim.2011.08.010

Rubtsov, A.V., K. Rubtsova, A. Fischer, R.T. Meehan, J.Z. Gillis, J.W. Kappler, and P. Marrack. 2011. Toll-like receptor 7 (TLR7)-driven accumulation of a novel CD11c+ B-cell population is important for the development of autoimmunity. *Blood.* 118:1305–1315. https://doi.org/10.1182/blood-2011-01-331462

Ruefli-Brasse, A.A., D.M. French, and V.M. Dixit. 2003. Regulation of NF-kappaB-dependent lymphocyte activation and development by paracaspase. *Science.* 302:1581–1584. https://doi.org/10.1126/science.1090769

Ruland, J., G.S. Duncan, A. Wakeham, and T.W. Mak. 2003. Differential requirement for Malt1 in T and B cell antigen receptor signaling. *Immunity.* 19:749–758. https://doi.org/10.1016/S1074-7613(03)00293-0

Sander, S., V.T. Chu, T. Yasuda, A. Franklin, R. Graf, D.P. Calado, S. Li, K. Imami, M. Selbach, M. Di Virgilio, et al. 2015. PI3 Kinase and FOXO1 Transcription Factor Activity Differentially Control B Cells in the Germinal Center Light and Dark Zones. *Immunity.* 43:1075–1086. https://doi.org/10.1016/j.immuni.2015.10.021

Schmitz, R., G.W. Wright, D.W. Huang, C.A. Johnson, J.D. Phelan, J.Q. Wang, S. Roulland, M. Kasbekar, R.M. Young, A.L. Shaffer, et al. 2018. Genetics and Pathogenesis of Diffuse Large B-Cell Lymphoma. *N. Engl. J. Med.* 378:1396–1407. https://doi.org/10.1056/NEJMoa1801445

Schwickert, T.A., H. Tagoh, K. Schindler, M. Fischer, M. Jaritz, and M. Busslinger. 2019. Ikaros prevents autoimmunity by controlling anergy and Toll-like receptor signaling in B cells. *Nat. Immunol.* 20:1517–1529. https://doi.org/10.1038/s41590-019-0490-2

Spandidos, A., X. Wang, H. Wang, and B. Seed. 2010. PrimerBank: a resource of human and mouse PCR primer pairs for gene expression detection and quantification. *Nucleic Acids Res.* 38(suppl_1):D792–D799. https://doi.org/10.1093/nar/gkp1005

Strasser, A., S. Whittingham, D.L. Vaux, M.L. Bath, J.M. Adams, S. Cory, and A.W. Harris. 1991. Enforced BCL2 expression in B-lymphoid cells prolongs antibody responses and elicits autoimmune disease. *Proc. Natl. Acad. Sci. USA.* 88:8661–8665. https://doi.org/10.1073/pnas.88.19.8661

Thome, M., J.E. Charton, C. Pelzer, and S. Hailfinger. 2010. Antigen receptor signaling to NF-kappaB via CARMA1, BCL10, and MALT1. *Cold Spring Harb. Perspect. Biol.* 2:a003004. https://doi.org/10.1101/cshperspect.a003004

Turner, M., and M.D. Díaz-Muñoz. 2018. RNA-binding proteins control gene expression and cell fate in the immune system. *Nat. Immunol.* 19:120–129. https://doi.org/10.1038/s41590-017-0028-4

Uehata, T., H. Iwasaki, A. Vandenbon, K. Matsushita, E. Hernandez-Cuellar, K. Kuniyoshi, T. Satoh, T. Mino, Y. Suzuki, D.M. Standley, et al. 2013. Malt1-induced cleavage of regnase-1 in CD4(+) helper T cells regulates immune activation. *Cell.* 153:1036–1049. https://doi.org/10.1016/j.cell.2013.04.034

Uren, A.G., K. O'Rourke, L.A. Aravind, M.T. Pisabarro, S. Seshagiri, E.V. Koonin, and V.M. Dixit. 2000. Identification of paracaspases and metacaspases: two ancient families of caspase-like proteins, one of which plays a key role in MALT lymphoma. *Mol. Cell.* 6:961–967. https://doi.org/10.1016/S1097-2765(00)00094-0

Victora, G.D., T.A. Schwickert, D.R. Fooksman, A.O. Kamphorst, M. Meyer-Hermann, M.L. Dustin, and M.C. Nussenzweig. 2010. Germinal center dynamics revealed by multiphoton microscopy with a photoactivatable fluorescent reporter. *Cell.* 143:592–605. https://doi.org/10.1016/j.cell.2010.10.032

Wei, J., L. Long, W. Zheng, Y. Dhungana, S.A. Lim, C. Guy, Y. Wang, Y.D. Wang, C. Qian, B. Xu, et al. 2019. Targeting REGNASE-1 programs long-lived effector T cells for cancer therapy. *Nature.* 576:471–476. https://doi.org/10.1038/s41586-019-1821-z

Werwitzke, S., D. Trick, K. Kamino, T. Matthias, K. Kniesch, B. Schlegelberger, R.E. Schmidt, and T. Witte. 2005. Inhibition of lupus disease by anti-double-stranded DNA antibodies of the IgM isotype in the (NZB x NZW)F1 mouse. *Arthritis Rheum.* 52:3629–3638. https://doi.org/10.1002/art.21379
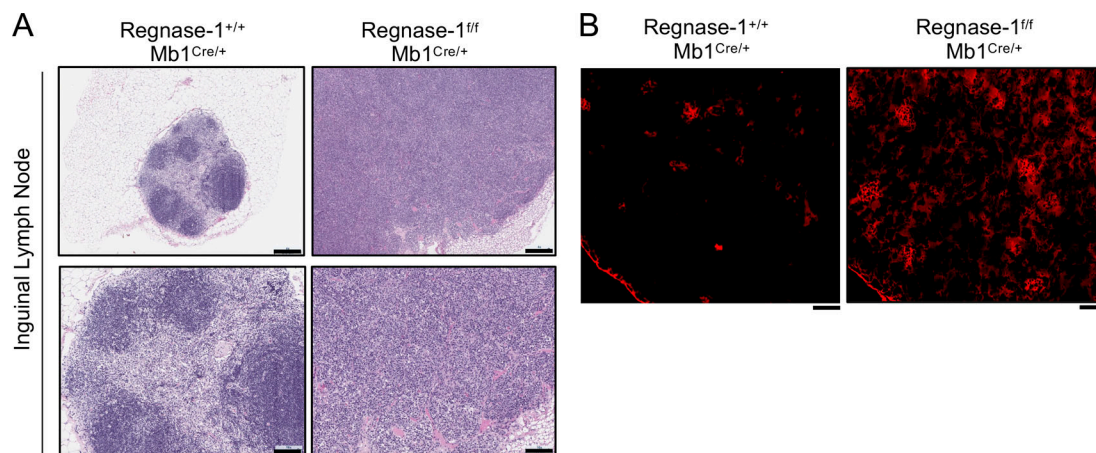
Figure S1. **Regnase-1 controls B cell–mediated immunopathology. (A)** H&E staining of the inguinal lymph nodes from mice of indicated genotypes. Scale bars = 250 μM (top), 100 μM (bottom); n = 3–5 mice; two independent experiments. **(B)** Representative immunofluorescence images of kidneys from 8–12-wk-old mice of indicated genotypes. Cryosections stained for total IgG (red); scale bar = 100 μM (n = 2 or 3 mice; two independent experiments).
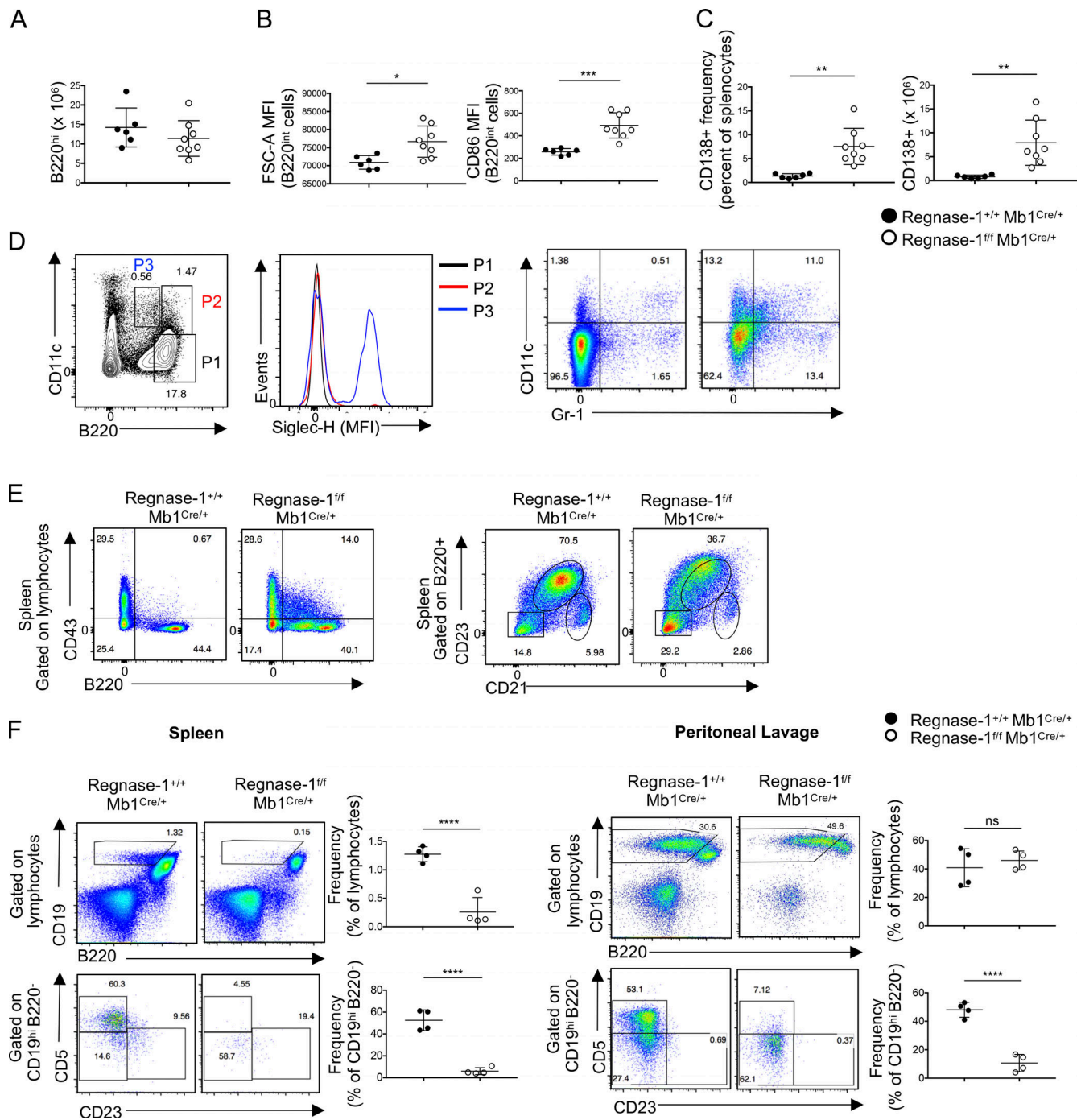
Figure S2. **Altered B cell populations in Regnase-1^f/f Mb1^Cre/+ mouse spleens. (A)** Absolute numbers of B220^hi B cells in spleens from mice of indicated genotypes. **(B)** Cell size (left) of B220^int B cells measured by forward scatter (FSC-A; left) and CD86 expression (right), both represented as MFI measured by flow cytometry. **(C)** Frequency (left) and total numbers (right) of CD138^+ cells in the spleens from mice of indicated genotypes assessed by flow cytometry. **(A–C)** Each circle represents an animal; solid circles = Regnase-1^+/+ Mb1^Cre/+, clear circles = Regnase-1^f/f Mb1^Cre/+; (*n* = 3–9 mice; at least three independent experiments). Horizontal lines indicate means with SD shown by error bars. Statistical significance calculated by unpaired Student's *t* test (*, P < 0.05; **, P < 0.01; ***, P < 0.001). **(D)** Representative flow cytometry dot plot (left) from spleen of Regnase-1^f/f Mb1^Cre mice showing B220 and CD11c staining gated as shown; CD11c and Gr-1 staining (right); and surface expression of Siglec-H from the indicated subpopulations represented as MFIs (middle; *n* = 3–9 mice; three independent experiments). **(E)** B220 and CD43 expression (left) on lymphocytes from spleens of indicated genotypes to show the presence of a CD43-expressing B cell subset in Regnase-1^f/f Mb1^Cre mice. Representative plots (right) showing altered CD21 and CD23 expression on B cells from Regnase-1^f/f Mb1^Cre mice. **(D and E)** *n* = 3–9 mice; two independent experiments. **(F)** Representative flow cytometry dot plot from spleen (left) and peritoneal lavage (right) from Regnase-1^f/f Mb1^Cre mice showing B1 cell subset frequencies using B220 and CD19 expression (top) and CD5 and CD23 expression (bottom) among cells gated on CD19^hiB220^lo population cells. Graphs showing combined data from two independent experiments (*n* = 2 in each experiment); ****, P < 0.0001. Horizontal lines indicate means with SD shown by error bars.
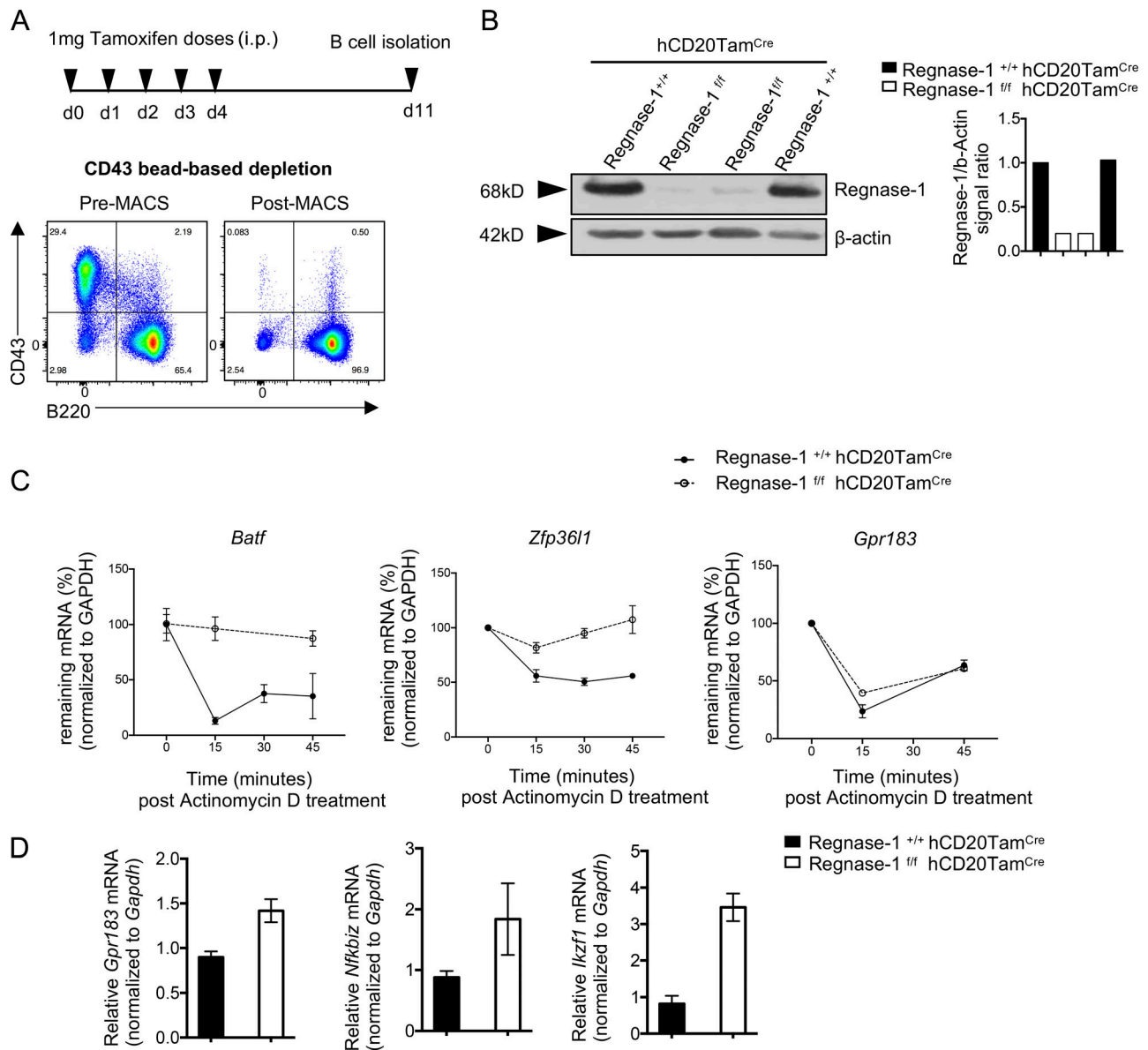
Figure S3. **Inducible deletion of Regnase-1 in B cells. (A)** Schematic indicating time points for tamoxifen administration and B cell isolation; flow cytometry plots showing purity of enriched B cells by CD43 magnetic bead–based depletion (n = 3–5 mice; at least two independent experiments). **(B)** Immunoblot showing deletion of Regnase-1 (left) and quantification of signal (right). Splenic B cells isolated on day 11 after tamoxifen dose #1. Each lane represents one animal (n = 2–5 mice; three independent experiments). **(C)** mRNA levels of *Batf* (left), *Zfp36l1* (middle), and *Gpr183* (right) in splenic B cells from mice of indicated genotypes at the indicated time points after actinomycin treatment (after anti-IgM stimulation). mRNA measured by RT-qPCR; relative abundance to GAPDH obtained for each data point, values normalized to untreated. n = 3 technical replicates; circles indicate means with SD shown by error bars. Data are representative of two independent experiments run using two mice from each genotype. **(D)** Fold change of total mRNA levels of *Gpr183* (left), *Nfkbiz* (middle), and *Ikzf1* (right) in unstimulated Regnase-1^f/f hCD20Tam^Cre B cells compared with Regnase-1^+/+ hCD20Tam^Cre controls. Bar graphs represent mean and standard deviation of fold changes from experimental triplicates from one animal (data represent two independent experiments; n = 2 in each). Expression levels of the tested transcripts have been normalized to levels of *GAPDH* mRNA control for each data point.
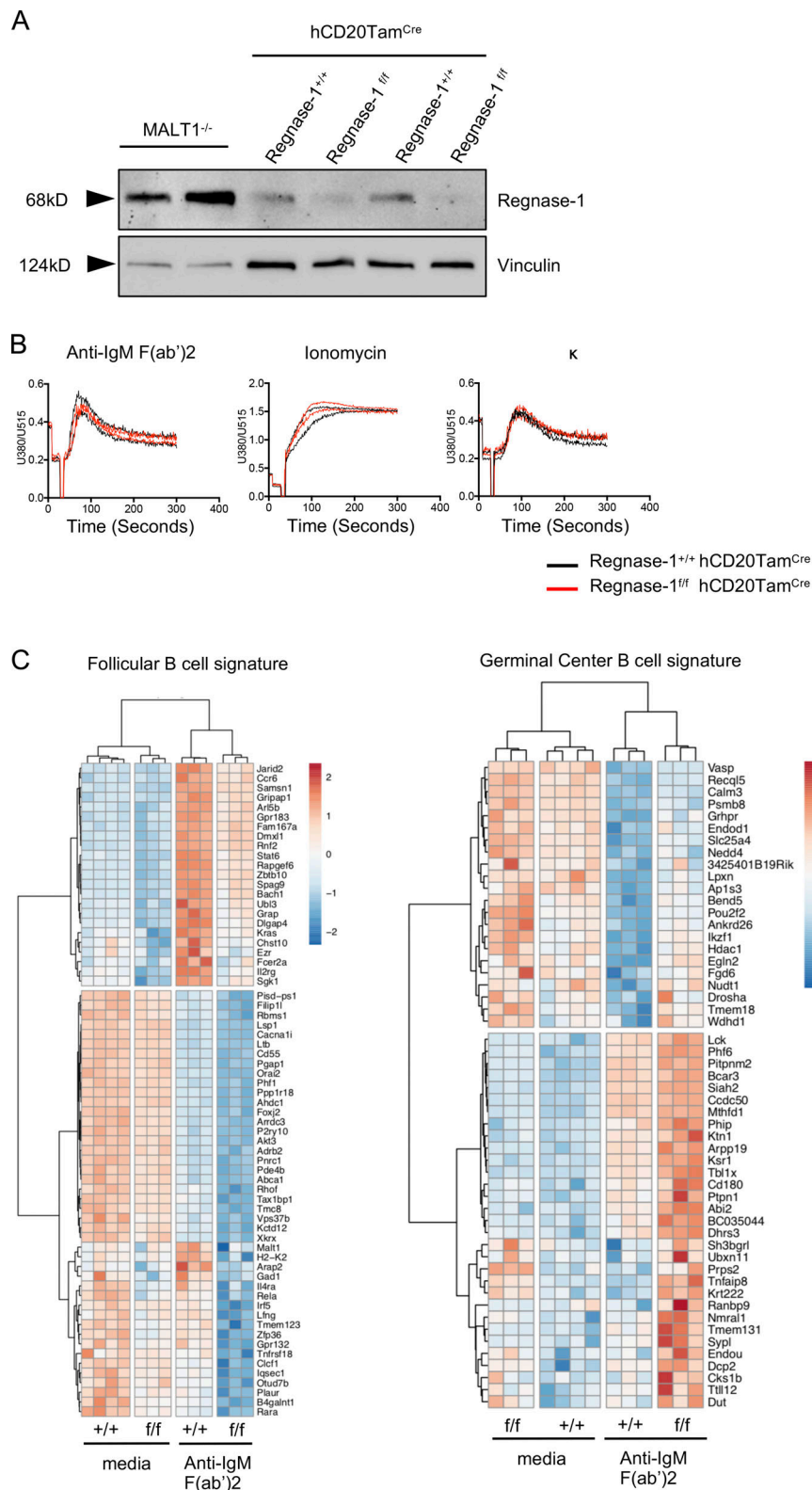
Figure S4. **Effect of Regnase-1 deletion on BCR signaling. (A)** Immunoblot comparing Regnase-1 protein expression in MALT1^{−/−} B cells to Regnase-1^{+/+} × hCD20[TamCre] Regnase-1[f/f] × hCD20[TamCre] B cells (each lane represents one animal; blot representative of two independent experiments). **(B)** Calcium flux in Regnase-1[f/f] hCD20Tam[Cre] and Regnase-1^{+/+} hCD20Tam[Cre] B cells upon indicated treatments, which include stimulatory anti-IgM and stimulatory anti-κ chain of BCR, with ionomycin treatment as positive control; measured by flow cytometry and shown as the ratio of calcium-bound to unbound indicator (n = 2 mice; two independent experiments). **(C)** Heatmaps showing the gene signatures of follicular (left) and GC (right) B cells that are significantly down-regulated or up-regulated in BCR-activated Regnase-1[f/f] hCD20Tam[Cre] B cells (n = 3 or 4 mice; RNA-seq experiment performed once). +/+, Regnase-1^{+/+} hCD20Tam[Cre] ; f/f, Regnase-1[f/f] hCD20Tam[Cre].

Provided online is one Excel table. Table S1 includes pathway and gene network analysis from the Metacore platform generated from the RNA-seq of Regnase-1–deficient B cells.